UNIVERSITÄTSKLINIKUM HAMBURG-EPPENDORF

Heinrich-Pette-Institut
Leibniz-Institut für Experimentelle Virologie
Abteilung Virus Immunologie

Wissenschaftlicher Direktor: Prof. Dr. Thomas Dobner

Eomes^{+} NK-Zellen als bedeutende Lymphozytenpopulation des angeborenen Immunsystems im Dünndarm von Neugeborenen

Publikationsdissertation

zur Erlangung des Grades eines Doktors der Medizin
an der Medizinischen Fakultät der Universität Hamburg.

vorgelegt von:

Adrian Friedrich Sagebiel
aus Hamburg

Hamburg 2020

Angenommen von der
Medizinischen Fakultät der Universität Hamburg am: 23.06.2021

Veröffentlicht mit Genehmigung der
Medizinischen Fakultät der Universität Hamburg.

Prüfungsausschuss, der/die Vorsitzende: Prof. Dr. Konrad Reinshagen

Prüfungsausschuss, zweite/r Gutachter/in: Prof. Marcus Altfeld

Prüfungsausschuss, dritte/r Gutachter/in: PD Dr. Jan de Laffolie

Inhaltsverzeichnis

Originalpublikation:

Originalpublikation:

Adrian F. Sagebiel, Fenja Steinert, Sebastian Lunemann, Christian Körner, Renée R.C.E. Schreurs, Marcus Altfeld, Daniel Perez, Konrad Reinshagen & Madeleine J. Bunders

Tissue-resident Eomes^{+} NK cells are the major innate lymphoid cell population in human infant intestine.

Nature Communications (2019)

nature COMMUNICATIONS

ARTICLE

https://doi.org/10.1038/s41467-018-08267-7 OPEN

Tissue-resident Eomes$^+$ NK cells are the major innate lymphoid cell population in human infant intestine

Adrian F. Sagebiel[1], Fenja Steinert[1], Sebastian Lunemann[1], Christian Körner[1], Renée R.C.E. Schreurs[2,3], Marcus Altfeld[1], Daniel Perez[4], Konrad Reinshagen[5] & Madeleine J. Bunders[1,2,3]

Innate lymphoid cells (ILC), including natural killer (NK) cells, are implicated in host-defense and tissue-growth. However, the composition and kinetics of NK cells in the intestine during the first year of life, when infants are first broadly exposed to exogenous antigens, are still unclear. Here we show that CD103$^+$ NK cells are the major ILC population in the small intestines of infants. When compared to adult intestinal NK cells, infant intestinal NK cells exhibit a robust effector phenotype, characterized by Eomes, perforin and granzyme B expression, and superior degranulation capacity. Absolute intestinal NK cell numbers decrease gradually during the first year of life, coinciding with an influx of intestinal Eomes$^+$ T cells; by contrast, epithelial NKp44$^+$CD69$^+$ NK cells with less cytotoxic capacity persist in adults. In conclusion, NK cells are abundant in infant intestines, where they can provide effector functions while Eomes$^+$ T cell responses mature.

[1] Department of Virus Immunology, Heinrich Pette Institute, Leibniz Institute for Experimental Virology, 20251 Hamburg, Germany. [2] Department of Experimental Immunology, Amsterdam Infection & Immunity Institute, Amsterdam University Medical Center, University of Amsterdam, 1105 AZ Amsterdam, The Netherlands. [3] Department of Pediatrics, Emma Children's Hospital, Amsterdam University Medical Center, University of Amsterdam, 1105 AZ Amsterdam, The Netherlands. [4] Department of General, Visceral and Thoracic Surgery, University Medical Center Hamburg-Eppendorf, 20246 Hamburg, Germany. [5] Department of Pediatric Surgery, University Medical Center Hamburg-Eppendorf, 20246 Hamburg, Germany. Correspondence and requests for materials should be addressed to M.J.B. (email: madeleine.bunders@leibniz-hpi.de)

Natural killer (NK) cells are innate lymphocytes that lack antigen-specific T or B cell receptors[1–4] and contain cytotoxic granules, providing them with the capacity to kill virus-infected cells[5]. NK cells have been classified as part of an heterogeneous group of innate lymphoid cells (ILCs) and play an important role in host-defense and tissue repair[6–9]. NK cells have superior cytotoxic qualities compared to other ILCs[10,11], which are generally identified by expression of the IL-7 receptor-α chain (CD127) and referred to as innate counterparts of T helper cells (ILC1s, ILC2s and ILC3s)[12,13]. However, NK cells and ILC1s do share the capacity to produce tumor necrosis factor-α (TNF-α) and interferon gamma (IFN-γ)[10,11]. Recent studies show that ILCs in tissues are able to provide local protection against infections[6,14]. ILCs and NK cells are already present in tissues early in human development and can be found in fetal intestines[15–17]. However, challenges to obtain infant tissues after birth have resulted in a lack of studies investigating NK cells during this critical phase of human development. As a result most of our understanding of NK cell ontogeny in children is based on studies of NK cells in blood or tissues derived from older children[18–20]. Therefore, the composition and kinetics of NK cells in intestines during the first year of life, when infants are exposed to exogenous antigens and have a high susceptibility to viral infections, are still unclear[21].

Here we demonstrate that CD127$^-$CD103$^+$Eomes$^+$ NK cells are the major ILC population in infant intestines during the first months of life, and that their absolute numbers decrease with age. Intestinal CD127$^+$ ILCs are also present early in life, but to a lesser extent than NK cells. Infant intestinal NK cells exhibit a cytotoxic phenotype compared with adult intestinal NK cells, and have higher perforin and granzyme B expression combined with superior capacity to degranulate. The number of intestinal NK cells and CD127$^+$ ILCs decreases as that of Eomes$^+$ T cells increases. Meanwhile, the intestinal NK cell subset persisting into adulthood is characterized by high expression of NKp44. Thus, the first year of life features dynamic changes in the lymphocyte compartment, shifting from Eomes$^+$ NK cells to Eomes$^+$ T cells in human intestines.

Results

Expression of NK cell markers on infant intestinal NK cells. ILCs are a heterogeneous population with different effector functions[6,9,10,12,17]. The lack of a hallmark lineage marker to distinguish NK cells from other ILC1s in tissues has led to conflicting results investigating ILCs[10,22–25]. Therefore, a detailed analysis of molecules expressed by NK cells, including CD16, CD56, CD127, CD7, KIR, CD94, NKp44, NKp46, NKp80, CD103, CD49a, and CD69 on viable CD45$^+$CD3$^-$CD14$^-$CD19$^-$ (lin$^-$) lymphocytes was performed. Flow cytometric data of intestinal epithelium, lamina propria, or peripheral blood-derived viable CD45$^+$lin$^-$ lymphocytes was analyzed by dimensional reduction using viSNE algorithm[26]. The unsupervised approach of viSNE resulted in a tissue-depended clustering of viable CD45$^+$lin$^-$ lymphocytes, indicating phenotypic differences between intestinal epithelial, lamina propria, and peripheral blood-derived cells (Fig. 1a). After dimensional reduction, intestinal epithelium, lamina propria, and blood-derived cells were highlighted separately to discern surface expression of signature molecules on viable CD45$^+$lin$^-$ lymphocytes (Fig. 1b). CD56 was frequently expressed on infant epithelium, lamina propria, and blood-derived viable CD45$^+$lin$^-$ lymphocytes. Intestinal epithelial CD56$^+$CD45$^+$lin$^-$ lymphocytes were detected in various cell clusters including CD127$^+$CD45$^+$lin$^-$ and CD127$^-$CD45$^+$lin$^-$ cells. The viSNE map of lamina propria-derived CD45$^+$lin$^-$ cells also showed CD127$^-$ and CD127$^+$CD56$^+$ hot spots. Thus, both CD127$^+$ ILCs and NK cells expressed CD56 and therefore CD56 alone could not be employed to distinguish NK cells from non-cytotoxic ILC1s without CD127. The Fcγ receptor IIIa (CD16), frequently used to identify NK cells in blood, was indeed highly expressed by infant blood CD45$^+$lin$^-$ cells, whereas only a small fraction of intestinal epithelial and lamina propria-derived CD45$^+$lin$^-$ lymphocytes expressed CD16. KIR expression is considered a hallmark of NK cells within the ILC family[10]. A small cluster of KIR$^+$CD56$^+$lin$^-$ cells was present in the intestinal epithelium and lamina propria of infants. CD127$^+$ cells were absent within the CD45$^+$lin$^-$KIR$^+$ cell cluster, verifying the exclusive expression of KIRs by NK cells. Next, we investigated whether other markers had a higher specificity to identify NK cells without requiring additional gating on CD127$^-$ cells. The NK cell receptor CD94, which together with NKG2A binds to HLA-E[2], was largely co-localized with CD56 on CD45$^+$lin$^-$ cells and was not detected within CD127$^+$ cell clusters. Gating on CD94$^+$CD45$^+$lin$^-$ cells however, did not include all KIR$^+$CD45$^+$lin$^-$ cell populations. A primary gating strategy based on CD94$^+$ cells would therefore exclude a proportion of epithelial and lamina propria-derived KIR$^+$ NK cells in infants. NKp80 is another surface marker that has been used to specifically identify NK cells[27]. Expression of NKp80 corresponded to a large extend to CD56 expression, however not all clusters identified by CD56 and CD94 were NKp80 positive, while at the same time there was overlap with CD127$^+$ cells, thus not providing better sensitivity and specificity. The natural cytotoxicity receptors (NCRs) NKp46 and NKp44 have been described on both NK cells and ILCs[28]. NKp46 included a large number of CD45$^+$lin$^-$ cell clusters, including KIR$^+$ cells, as well as CD127$^+$lin$^-$ cells from infant intestines, demonstrating that this NCR did not improve the selectivity of a gating strategy based on CD56 and CD127. The expression of NKp44 was less abundant than NKp46 on intestinal epithelium or lamina propria-derived CD45$^+$lin$^-$ cells. However, CD127$^+$ and CD127$^-$ clusters were distinguished amongst NKp44$^+$ cells from infant epithelial and lamina propria tissues, eliminating NKp44 as a lineage marker for NK cells. Taken together, a gating strategy based on CD56$^+$CD45$^+$lin$^-$ cells and excluding CD127$^+$ cells (Fig. 2a) included all KIR$^+$lin$^-$lymphocytes as well as NK cell populations identified by other markers, such as NKp80 and CD94 (Fig. 1b). Applying this gating strategy showed that CD16 expression by infant intestinal epithelial NK cells was low compared to infant peripheral blood cells, with only 16% (median, interquartile ranges (IQR) 11–21%) of infant epithelial NK cells expressing CD16 (Fig. 2a, c, Supplementary Fig. 1). Similar small frequencies of CD16$^+$ NK cells were detected in adult small intestinal tissues. In conclusion, NK cells derived from infant blood and intestines differed significantly in their expression of hallmark surface markers. We furthermore established a gating strategy of CD127$^-$CD56$^+$CD45$^+$lin$^-$ cells that allowed for a comprehensive characterization of NK cells in infant intestines.

NK cells form the major ILC population in infant intestines. Using the gating strategy established above, the contribution of viable CD127$^-$CD56$^+$CD45$^+$lin$^-$ lymphocytes (hereafter called NK cells) to overall lymphocyte populations in infant intestines was quantified. In infants under 3 months of age, NK cells comprised a large proportion of epithelial (median 29%, IQR 17–35%) and lamina propria-derived (median 15%, IQR 8–26%) lymphocytes. In contrast, NK cells contributed only 4% (median, IQR 2–6%) to epithelial lymphocytes and 1% (median, IQR 1–2%) to lymphocytes in the lamina propria of adult intestines (Fig. 2d). Absolute NK cell numbers decreased after ~6 months of age (Fig. 2e, Supplementary Fig. 1). Intestines of infants under

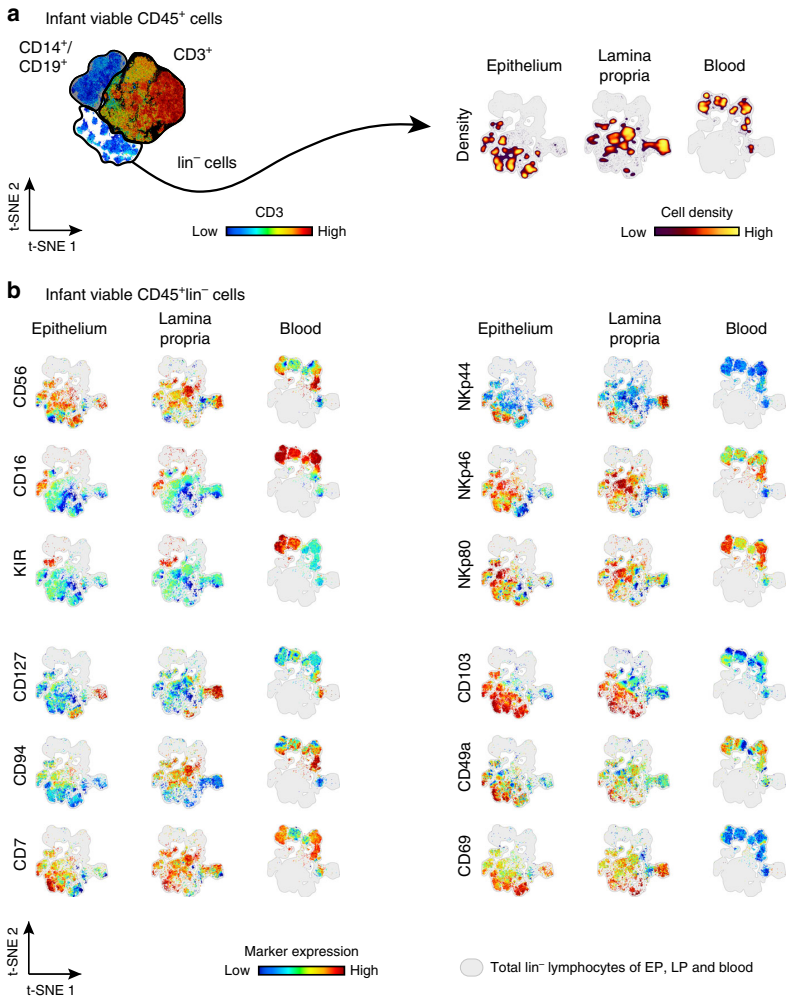

Fig. 1 Hallmarks of ILCs by infant blood and intestinal CD45$^+$lin$^-$ cells. **a** viSNE plot of flow cytometric analysis of viable CD45$^+$ cells showing separate clustering by tissue of origin: epithelium (EP), lamina propria (LP), and blood (B). **b** Individual representation of hallmarks of ILCs (CD56, CD16, KIR, CD127, CD94, CD7, NKp44, NKp46, NKp80, CD103, CD49a, and CD69) using viSNE algorithm of flow cytometric data of lin$^-$(CD14$^-$CD19$^-$CD3$^-$) cells for EP, LP, and blood samples. Expression is shown by color coding in relative intensity. viSNE plots have been calculated from concatenated FCS files gated on viable CD45$^+$ lymphocytes from epithelium, lamina propria, and blood of matched donors ($N = 4$, iterations = 7500 perplexity = 100, KL divergence = 2.15)

6 months of age contained 51,103 epithelial NK cells (median, IQR 44,198–69,504) per cm^2 compared to 2877 epithelial NK cells (median, IQR 2092–3819) in adult intestines. Absolute counts of lamina propria-derived NK cells/cm^2 decreased from 78,620 (median, IQR 39,274–112,743) in infants under 6 months of age to 4941 (median, IQR 3449—9762) in adults (Fig. 2e). Intestinal CD127$^+$ ILCs showed a similar trend over age as NK cells. The highest absolute numbers and frequencies of epithelial and lamina propria-derived CD127$^+$ ILCs were detected after birth and decreased thereafter (Supplementary Fig. 1). NK cell frequencies and absolute numbers remained higher compared to CD127$^+$ ILCs in intestines during infancy (Fig. 2d, e and Supplementary Fig. 1). Taken together, intestines of infants after birth contained 17.8 times more epithelial ($p < 0.001$) and 15.9 times more lamina propria-derived ($p < 0.001$) NK cells, respectively, compared to adult intestines, indicating that NK cells are amongst the most numerous lymphocytes in intestines early in life.

Infant intestinal NK cells have a tissue-residency phenotype. Tissue-resident lymphocytes, including ILCs, allow for compartmentalization of immune responses adapted to local requirements[29–33]. CD69, CD103, and CD49a have been suggested to facilitate retention of lymphocytes in intestinal tissues[29–32]. Epithelial NK cells showed high expression of CD103 both in infant (median 90%, IQR 80–92%) and adult intestines (median 93%, IQR 78–97%) (Fig. 3a, b). Infant lamina propria-derived NK cells however exhibited a higher expression of CD49a compared to adult NK cells ($p = 0.003$). In line, viSNE plots showed absence of CD49a expression in those clusters with the highest density of adult lamina propria-derived NK cells (upper right location of the viSNE map) (Fig. 3a). In contrast, CD69 was expressed significantly lower on infant epithelial and lamina propria-derived NK cells compared to adult NK cells ($p < 0.001$ and $p < 0.001$, respectively) (Fig. 3b). Of note, CXCR6, identifying tissue-resident NK cells in the liver[34], was relatively rarely expressed

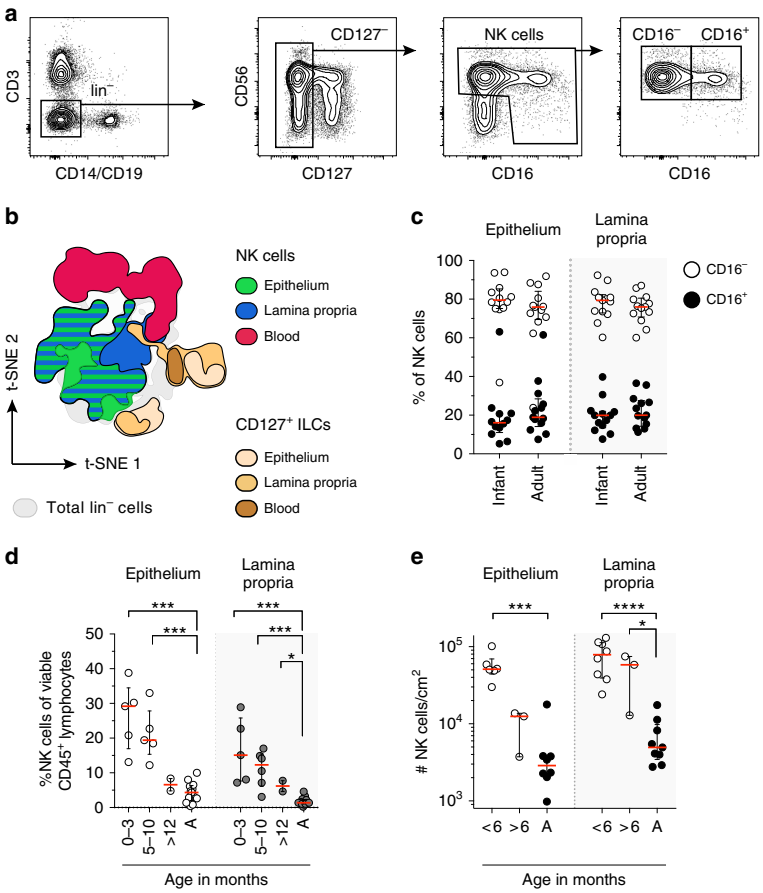

Fig. 2 NK cells are abundant in infant intestines. **a** Flow cytometric plots showing the applied gating strategy for intestinal NK cells (viable CD56$^+$CD127$^-$ CD45$^+$lin$^-$ cells). FACS plots of a representative donor are shown. **b** viSNE plot of flow cytometric data showing gated NK cells and CD127$^+$ ILCs from epithelium (EP), lamina propria (LP) and blood (B) within lin$^-$ populations (gray) ($N = 4$). **c** Frequencies of infant and adult CD16$^-$ (white circles) and CD16$^+$ (black circles) NK cells from EP ($N = 12$) and LP ($N = 13$) tissues (infant samples), adult samples $N = 13$ (EP and LP). **d** NK cell frequencies of viable lymphocytes shown for different age groups in EP and LP tissues (infant samples $N = 12$ (EP) and $N = 13$ (LP), adult samples (A) $N = 13$ (EP and LP). **e** Absolute NK cell numbers per cm^2 for different age groups in EP and LP tissues (infant samples $N = 9$ (EP) and $N = 11$ (LP), adult samples (A) $N = 8$ (EP), and $N = 9$ (LP)). Median frequencies indicated by red lines. Error bars define interquartile ranges between 75th and 25th percentiles. Statistical comparisons are Mann-Whitney U comparisons. Asterisks represent the following p-values: *$p < 0.05$; ***$p < 0.001$; and ****$p < 0.0001$

on intestinal NK cells compared to CD103 or CD69 (Supplementary Fig. 2). Taken together, the majority of intestinal NK cells early in life were CD103$^+$ phenotypic tissue-resident NK cells. Furthermore, CD69 expression was significantly lower on infant intestinal NK cells and increased with age.

Infant intestinal NK cells have high NKG2A expression. Expression of NKG2A, KIR, and CD57 has been suggested to track NK cell differentiation, with NKG2A levels decreasing while KIR and CD57 increase upon maturation[35]. viSNE analyses showed NKG2A-positive and KIR-positive clusters of infant epithelium and lamina propria-derived NK cells. Remarkably, NKG2A and KIR were co-expressed in a small cluster in the upper left area of the viSNE map, while CD57$^+$ cells were scarce and did not form a separate cluster (Fig. 4a). NKG2A$^+$ NK cells were 1.8-fold and 1.4-fold more frequent in epithelium ($p = 0.003$) and lamina propria ($p = 0.002$) of infant intestines, respectively, compared to adult intestines (Fig. 4b). Although higher NKG2A expression by infant NK cells suggested a more immature phenotype, frequencies of KIR$^+$ NK cells in infant intestines were also significantly higher compared to adult NK cells (Fig. 4b). Thus, expression of NKG2A and KIR significantly differed between adult and infant intestinal NK cells. Frequencies of CD57$^+$ infant and adult intestinal NK cells were low (Supplementary Fig. 3). Next, we assessed expression of NKG2A and KIR on CD103$^+$, CD49a$^+$, or CD69$^+$ NK cells derived from infant and adult intestines. NKG2A was significantly higher expressed on CD103$^+$ and CD49a$^+$ infant intestinal NK cells than on CD69$^+$ NK cells (NKG2A expression on CD103$^+$ vs. CD69$^+$ epithelial NK cells: $p = 0.002$; NKG2A expression on infant CD49a$^+$ vs. CD69$^+$ lamina propria-derived NK cells: $p = 0.008$) (Fig. 4c, d). Moreover, intestinal epithelial and lamina propria-derived KIR$^+$ NK cells were also significantly reduced in CD69$^+$ compared to CD103$^+$ NK cell populations (Fig. 4c, d). Overall, these data suggest that intestinal NK cells have a relatively immature phenotype; however, a KIR$^+$ NK cell population is present, in particular in infant intestines. We next investigated

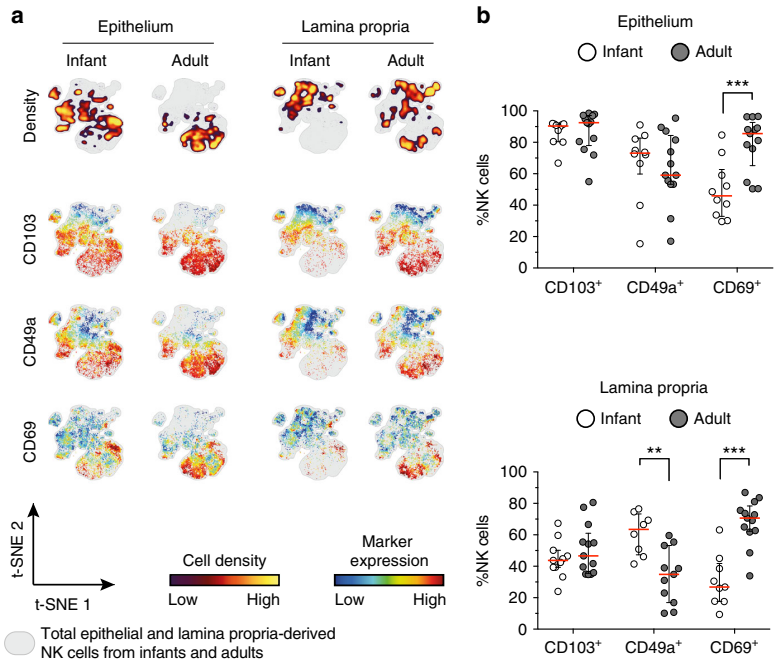

Fig. 3 Intestinal NK cells express tissue-residency markers. **a** viSNE plots of combined flow cytometric data visualizing CD103, CD49a, and CD69 expression on infant and adult NK cells from epithelium (EP) and lamina propria (LP) intestinal tissues. Cell density of clusters is shown in first row. Expression patterns of tissue-residency markers CD103, CD49a, and CD69 are depicted by color coding in relative intensity in following plots. viSNE plots have been calculated from concatenated FCS files gated on NK cells (infant samples $N = 9$, adult samples $N = 6$, iterations = 7500 perplexity = 100, KL divergence = 2.29). **b** Frequencies of epithelial and lamina propria-derived CD103$^+$, CD49a$^+$, or CD69$^+$ NK cells from infant (white circles) and adult intestines (dark circles) (EP infant samples ($N = 10$), EP adult samples ($N = 13$), LP infant samples (CD103 ($N = 11$), CD69 ($N = 9$), CD49a ($N = 8$), LP adult samples (CD103 ($N = 13$), CD69 ($N = 13$), CD49a ($N = 11$)). Median frequencies indicated by red lines. Error bars define interquartile ranges between 75th and 25th percentiles. Statistical comparisons are Mann-Whitney *U* comparisons. Asterisks represent the following *p*-values: $^{**}p < 0.01$ and $^{***}p < 0.001$

whether hallmark nuclear transcription factors for ILC and NK cell development might contribute to the differential NK cell phenotypes observed in infants and adults.

Eomes$^+$ NK cells are abundant in infant intestines. The T-box transcription factors Eomesodermin (Eomes) and TBX21 (T-bet) are both essential for NK cell development. Whereas Eomes is more restricted to NK cell development, T-bet is also critical for induction and lineage-commitment of CD127$^+$ ILCs[12]. Tissue-resident NK cells in livers have been described to be Eomes^{high} and T-bet^{low}[36,37]. Our analyses of infant intestines showed large clusters of epithelial Eomes$^+$ NK cells in viSNE graphs, whereas adult epithelial Eomes$^+$ NK cells were scarce (Fig. 5a). Quantitative analyses showed that 49% (median, IQR 38–69%) of infant epithelial NK cells and 86% (median, IQR 78–91%) of infant lamina propria-derived NK cells were Eomes$^+$, 2.2-fold and 1.9-fold higher compared to adults ($p = 0.003$ and $p < 0.001$, respectively) (Fig. 5b). Infant intestinal NK cells were T-bet^{low} with only 12% (median, IQR 7–24%) of infant epithelial and 15% (median, IQR 10–26%) of lamina propria-derived NK cells expressing T-bet (Supplementary Fig. 4). The number of T-bet$^+$ NK cells was further decreased in adult intestines. Furthermore, Eomes expression by intestinal NK cells differed between CD103$^+$ and CD69$^+$ cells, as CD103$^+$ NK cells expressed significantly more Eomes compared to CD69$^+$ NK cells (Fig. 5c, d). This was observed for infant intestinal epithelial NK cells ($p = 0.008$) as well as infant ($p = 0.02$) and adult ($p = 0.04$) lamina propria-derived NK cells (Fig. 5d). Taken together, a significantly larger population of tissue-resident NK cells with high expression of Eomes was present in infant compared to adult intestines, with the highest Eomes expression detected amongst infant CD103$^+$ NK cells, while Eomes expression among infant intestinal CD69$^+$ NK cells was low.

Superior functional capacity of infant intestinal NK cells. Eomes$^+$ NK cells are generally considered exemplar NK cells with the capacity to induce cytotoxicity upon release of granzyme B-containing and perforin-containing granules[10]. Approximately 54% (median, IQR 25–76%) of infant epithelial NK cells contained perforin, which was four times more ($p = 0.01$) than adult epithelial NK cells (median 12%, IQR 7–21%) (Fig. 6a, b). Furthermore, the majority of infant lamina propria-derived NK cells (median 68%, IQR 36–82%) contained perforin compared to 24% (median, IQR 14–43%) in adult intestines ($p = 0.008$). A similar trend was observed for granzyme B, with higher frequencies of granzyme B$^+$ infant than adult intestinal NK cells (epithelium $p = 0.04$, lamina propria $p < 0.001$) (Fig. 6b). viSNE analyses of infant and adult donors further revealed co-expression of Eomes and KIR with perforin and granzyme B (Fig. 6a). Analogous to Eomes, infant epithelial CD103$^+$ NK cells had significantly higher levels of perforin ($p = 0.02$) and granzyme B ($p = 0.008$) compared to CD69$^+$ NK cells (Fig. 6c). Furthermore, infant epithelial CD49a$^+$ NK cells contained significantly more granzyme B compared to CD69$^+$ NK cells ($p = 0.008$). A similar pattern was observed when comparing lamina propria-derived CD103$^+$ and CD69$^+$ NK cells (Fig. 6c). The consistent lower expression of

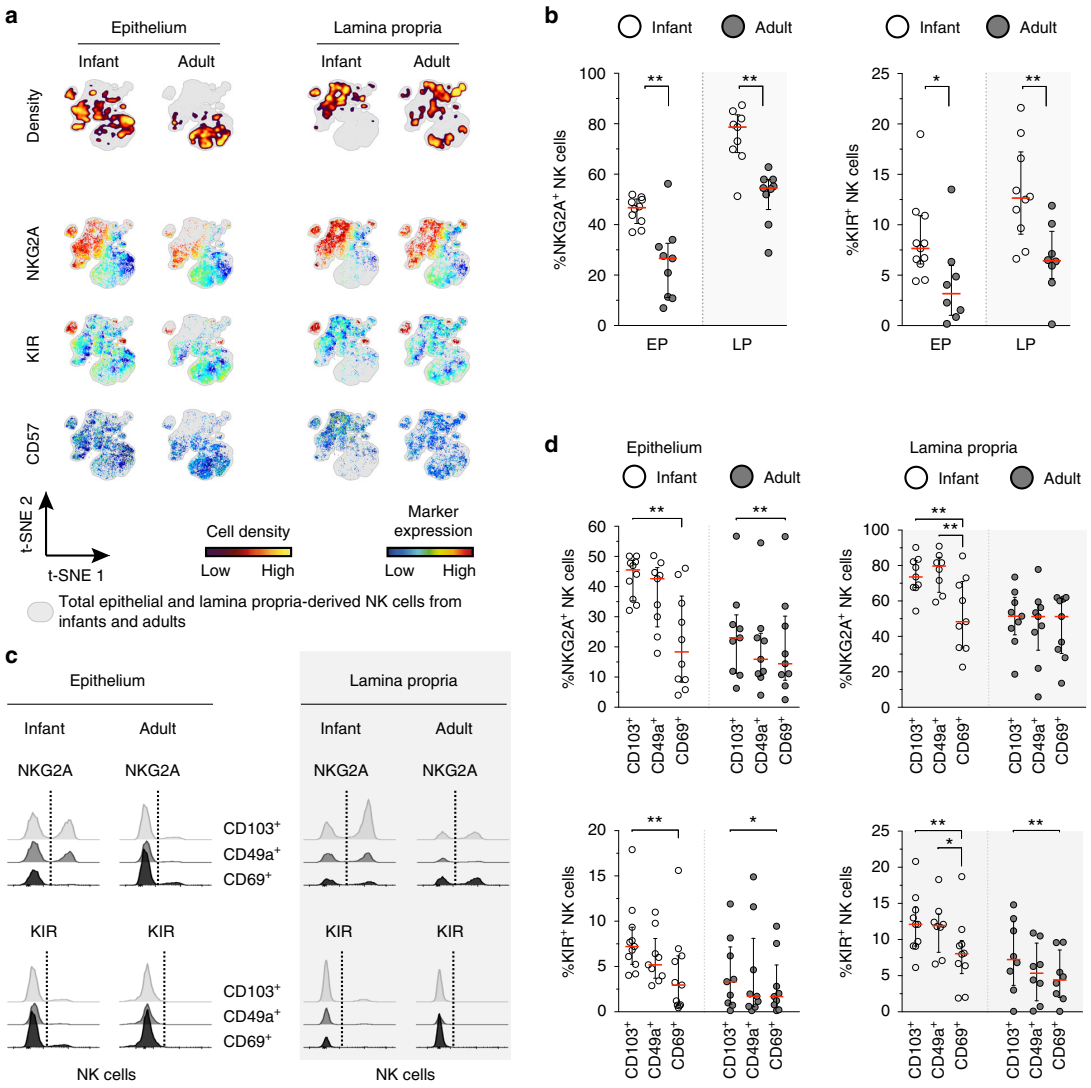

Fig. 4 Infant intestinal NK cells have high NKG2A expression. **a** viSNE plots of combined flow cytometric data visualizing NKG2A, KIR, and CD57 expression by infant and adult epithelial (EP) and lamina propria-derived (LP) NK cells. Cell density of clusters is shown in first row. The expression of NKG2A, KIR, and CD57 is shown by color coding in relative intensity below. viSNE plots are calculated from concatenated FCS files gated on NK cells (infant samples $N = 9$, adult samples $N = 6$, iterations = 7500 perplexity = 100, KL divergence = 2.29). **b** Frequencies of epithelial and lamina propria-derived infant (white circles) and adult (dark circles) NKG2A$^+$ NK cells and KIR$^+$ NK cells (EP infant samples NKG2A ($N = 10$), KIR ($N = 11$), LP infant samples NKG2A ($N = 9$), KIR ($N = 10$), EP adult samples NKG2A ($N = 9$), KIR ($N = 8$), LP adult samples NKG2A ($N = 9$), KIR ($N = 8$)). **c** Histogram overlay of flow cytometric data showing NKG2A and KIR expression by CD103$^+$ (gray), CD49a$^+$ (dark gray), and CD69$^+$ (black) NK cells from infant and adult intestines. **d** Frequencies of infant (white circles) and adult (dark circles) intestinal NKG2A$^+$ NK cells and KIR$^+$ NK cells within CD103$^+$, CD49a$^+$, or CD69$^+$ populations. NKG2A expression by infant EP CD103$^+$ ($N = 10$), CD69$^+$ ($N = 10$), and CD49a$^+$ ($N = 9$) NK cells, NKG2A expression by infant LP-derived CD103$^+$ ($N = 9$), CD69$^+$ ($N = 9$), and CD49a$^+$ ($N = 8$) NK cells. NKG2A expression by adult EP and LP-derived NK cells ($N = 9$). KIR expression by infant EP CD103$^+$ ($N = 11$), CD69$^+$ ($N = 11$), and CD49a$^+$ ($N = 9$) NK cells. KIR expression by infant LP-derived CD103$^+$ ($N = 10$), CD69$^+$ ($N = 10$), and CD49a$^+$ ($N = 8$) NK cells. KIR expression by adult EP ($N = 9$) and LP-derived ($N = 8$) NK cells. Median frequencies indicated by red lines. Error bars define interquartile ranges between 75th and 25th percentiles. Statistical comparisons are Mann-Whitney *U* comparisons (**b**) and Wilcoxon matched-pairs signed rank tests (**d**). Asterisks represent the following *p*-values: $*p < 0.05$ and $**p < 0.01$

granzyme B and perforin in infant CD69$^+$ NK cells compared to CD103$^+$ NK cells was not observed for adult epithelial NK cells, as almost all adult epithelial NK cells were double positive for CD103 and CD69 (Fig. 3b). However, adult CD103$^+$ NK cells and CD69$^+$ NK cells were present in the lamina propria and a significant difference was detected between CD103$^+$ and CD69$^+$ NK cells (Fig. 6c). Taken together, these data show that infant intestinal NK cells, and in particular CD103$^+$CD69$^-$ NK cells, contained more granzyme B and perforin than adult intestinal NK cells.

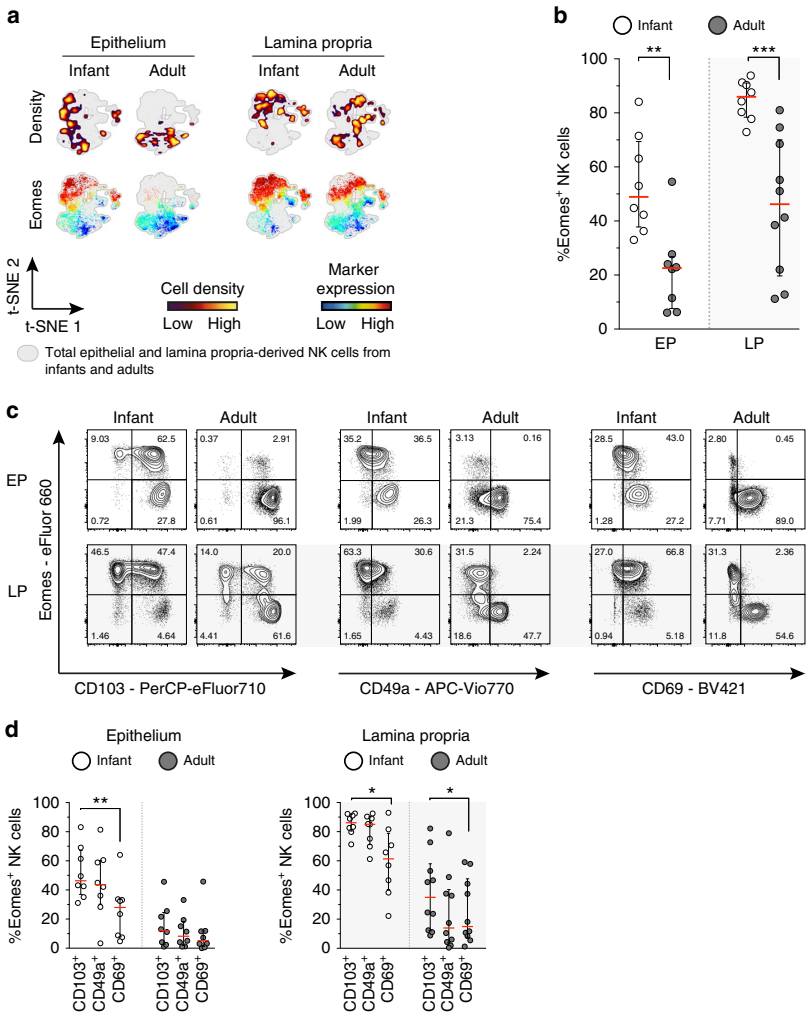

Fig. 5 High expression of Eomes in infant intestinal NK cells. **a** viSNE plots of combined flow cytometric data visualizing Eomes expression of infant and adult NK cells from epithelium (EP) and lamina propria (LP) intestinal tissues. Cell density of clusters is shown in first row. Expression of Eomes is shown by color coding in relative intensity in second row. viSNE plots have been calculated from concatenated FCS files gated on NK cells (infant samples $N = 7$, adult samples $N = 5$, iterations = 7500 perplexity = 100, KL divergence = 2.62). **b** Frequencies of EP and LP-derived infant (white circles) and adult (dark circles) Eomes$^+$ NK cells. **c** Representative flow cytometric plots showing co-expression of Eomes and tissue-residency markers (CD103, CD49a, CD69) in NK cells from EP and LP of infant and adult intestines. **d** Frequencies of Eomes$^+$ NK cells within CD103$^+$, CD49a$^+$, or CD69$^+$ NK cell populations in EP and LP of infants (white circles) and adults (dark circles) (infant samples $N = 8$ (EP and LP), adult samples $N = 8$ (EP), and $N = 10$ (LP)). Median frequencies indicated by red lines. Error bars define interquartile ranges between 75th and 25th percentiles. Statistical comparisons are Mann-Whitney *U* comparisons (**b**) and Wilcoxon matched-pairs signed rank tests (**d**). Asterisks represent the following *p*-values: $*p < 0.05$; $**p < 0.01$; and $***p < 0.001$

The function of infant and adult intestinal NK cells was further assessed using degranulation and cytokine production assays. Due to low numbers of adult epithelial NK cells in intestines, these functional analyses were only performed using lamina propria-derived NK cells for comparisons. After isolation, lymphocytes were stimulated with phorbol-12-myristate-13-acetate (PMA) and ionomycin, K562 or 772.221 target cell lines. In infants, 77% (median, IQR 65–78%) of NK cells expressed CD107a upon stimulation with PMA and ionomycin, while only 54% (median, IQR 49–65%) of adult NK cells expressed CD107a ($p = 0.02$). Stimulation with PMA and ionomycin resulted in IFN-γ production by 43% (median, IQR 39–56%) of infant intestinal NK cells and 19% (median, IQR 18–54%) of adult intestinal NK cells, whereas TNF-α was produced by 23% (median, IQR 8–50%) of infant and 9% (median, IQR 3–19%) of adult intestinal NK cells (Fig. 6d). After stimulation with K562 or 772.221 target cell lines, infant lamina propria-derived NK cells showed a trend towards enhanced degranulation compared to adult NK cells (Supplementary Fig. 5). Even though CD107a expression was relatively high on all NK cells, differential effects were observed between CD103$^+$ and CD69$^+$ NK cells (Fig. 6e). In particular adult intestinal CD69$^+$ NK cells showed a significant lower level of degranulation compared to CD103$^+$ NK cells ($p = 0.03$) (Fig. 6e), and a similar trend was observed for infant NK cells ($p = 0.06$). In conclusion, infant intestinal NK cells contained significantly more cytotoxic molecules and showed

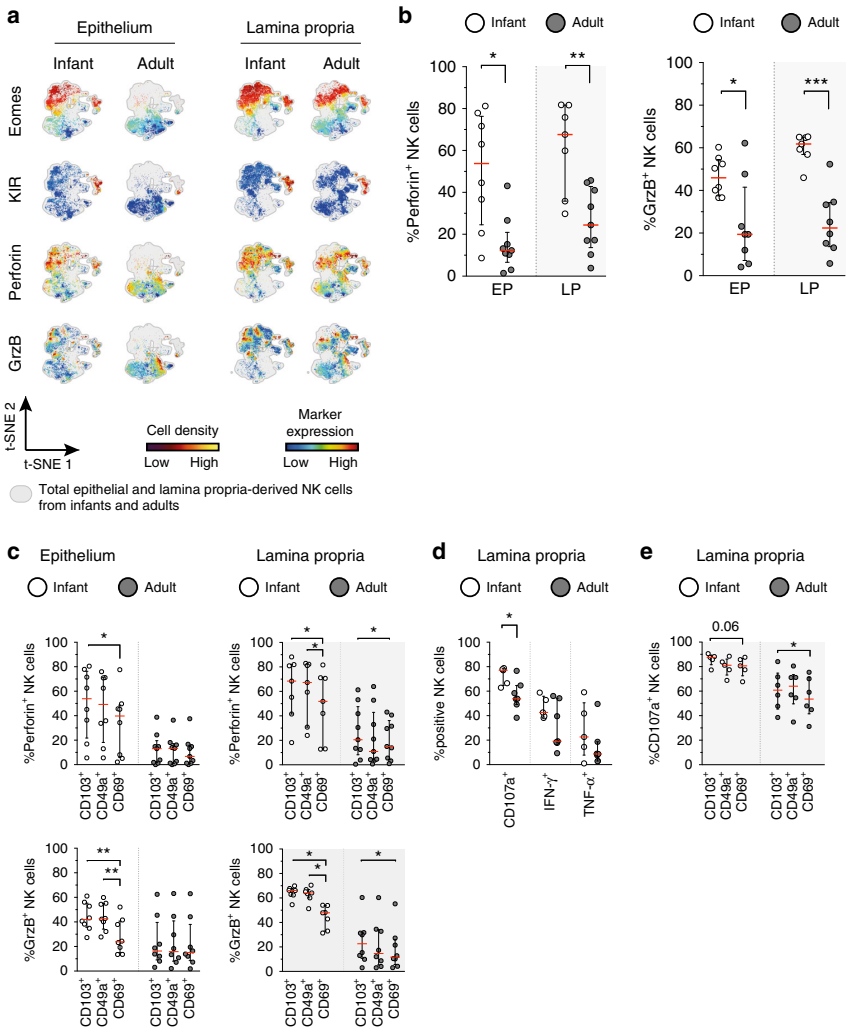

Fig. 6 Infant intestinal NK cells contain high levels of cytotoxic granules. **a** viSNE plots of combined flow cytometric data visualizing Eomes, perforin, granzyme B, and KIR expression by epithelial (EP) and lamina propria-derived (LP) infant and adult NK cells. Expression of Eomes, KIR, perforin, and granzyme B (GrzB) is shown by color coding in relative intensity. viSNE plots have been calculated from concatenated FCS files gated on NK cells (infant samples $N = 7$, adult samples $N = 5$, iterations = 7500 perplexity = 100, KL divergence = 2.62). **b** Frequencies of perforin$^+$ and GrzB$^+$ NK cells in infants (white circles) and adults (dark circles) (EP infant samples ($N = 8$), LP infant samples ($N = 7$), EP adult samples perforin expression ($N = 9$), GrzB expression ($N = 8$), LP adult samples perforin expression ($N = 9$), and GrzB expression ($N = 8$)). **c** Frequencies of perforin$^+$ and granzyme B$^+$ cells within CD103$^+$, CD49a$^+$, or CD69$^+$ NK cell populations in infant (white circles) and adult intestines (dark circles) (EP infant samples ($N = 8$), LP infant samples ($N = 7$), EP adult samples perforin expression ($N = 9$), and GrzB expression ($N = 8$), LP adult samples perforin expression ($N = 9$), and GrzB expression ($N = 8$)). **d** Frequencies of LP-derived CD107a$^+$, IFN-γ$^+$, and TNF-α$^+$ NK cells in infant (white circles) and adult intestines (dark circles). Cells were stimulated for 6 h with phorbol 12-myristate 13-acetate (PMA) and ionomycin (infant samples $N = 5$, adult samples $N = 7$). **e** Frequencies of LP-derived CD107a$^+$ cells within CD103$^+$, CD49a$^+$, or CD69$^+$ NK cell populations in infant (white circles) and adult intestines (dark circles) after stimulation with PMA and ionomycin for 6 h (infant samples $N = 5$, adult samples $N = 6$). Median frequencies indicated by red lines. Error bars define interquartile ranges between 75th and 25th percentiles. Statistical comparisons are Mann-Whitney *U* comparisons (**b**, **d**) and Wilcoxon matched-pairs signed rank tests (**c**, **e**). Asterisks represent the following *p*-values: $*p < 0.05$; $**p < 0.01$; and $***p < 0.001$

superior degranulation upon stimulation than adult intestinal NK cells.

CD103$^+$NKp44$^+$CD127$^-$lin$^-$ cells persist in adult intestines. Our studies observed a highly dynamic intestinal NK cell compartment during childhood with an abundance of intestinal NK cells early in life followed by their rapid decrease. Recently, epithelial CD103$^+$NKp44$^+$ ILC1s were described in intestines of adults, which also exhibited certain features of NK cells, such as IFN-γ production and perforin expression[38,39]. We confirmed that epithelial NK cells in adult intestines expressed NKp44 (median 67%, IQR 54–72%) (Fig. 7a), whereas in infant intestines the percentage of epithelial NKp44$^+$ NK cells was significantly

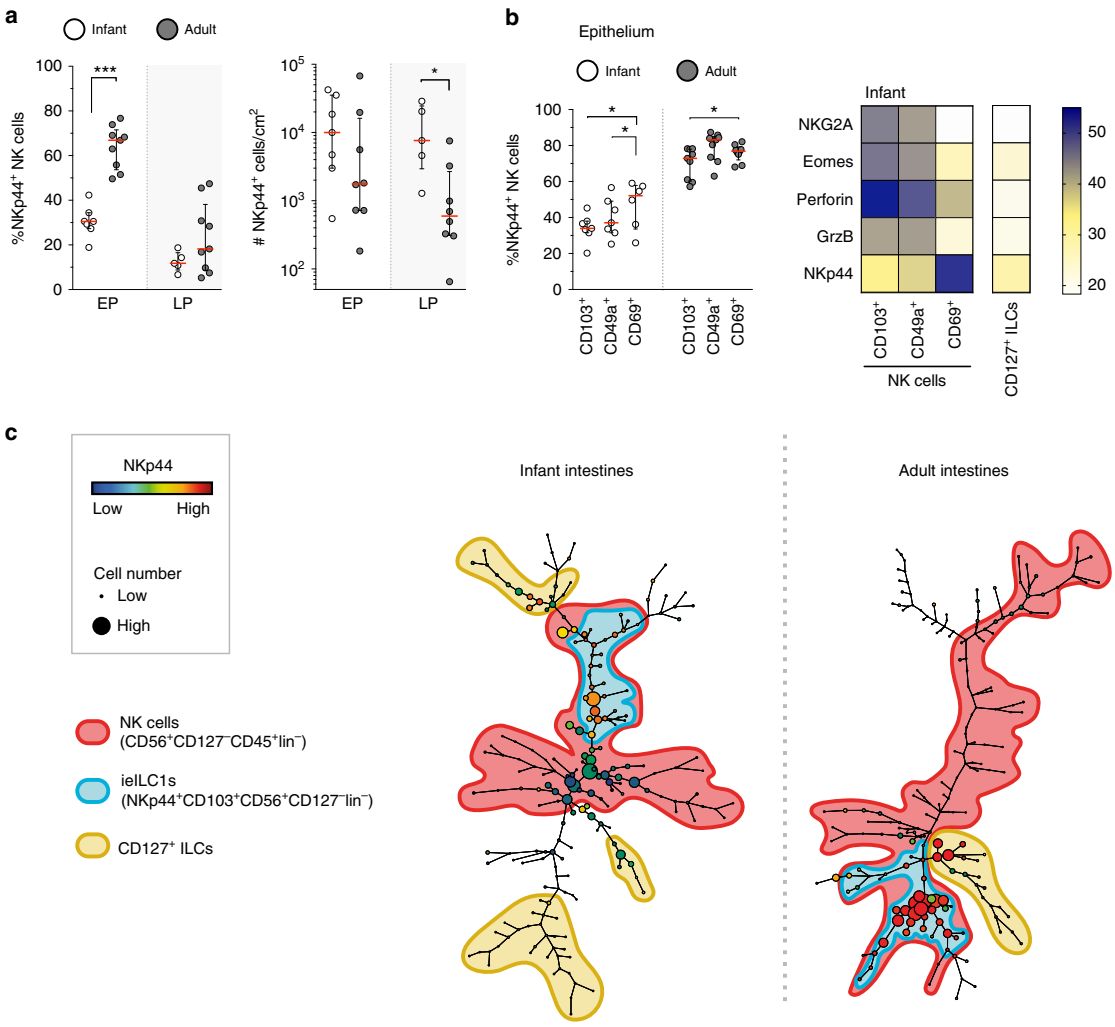

Fig. 7 Epithelial CD103$^+$NKp44$^+$lin$^-$ cells are the major ILC population in adults. **a** Frequencies as well as absolute cell numbers per cm^2 of epithelial (EP) and lamina propria-derived (LP) NKp44$^+$ NK cells in infant (white circles) and adult (dark circles) intestines (infant NK cell frequencies and absolute counts EP ($N = 7$) and LP ($N = 5$), adult NK cell frequencies ($N = 9$) and absolute counts ($N = 8$)). **b** Frequencies of NKp44$^+$ cells within CD103$^+$, CD49a$^+$, or CD69$^+$ NK cells in infants (white circles) and adults (dark circles). NKp44 expression by infant epithelial CD103$^+$ ($N = 7$), CD49a$^+$ ($N = 7$), and CD69$^+$ ($N = 6$) NK cells. NKp44 expression by adult epithelial NK cell subsets ($N = 9$). Heatmap of median frequencies of NKG2A$^+$, Eomes$^+$, perforin$^+$, granzyme B$^+$, and NKp44$^+$ cells within CD103$^+$, CD49a$^+$, or CD69$^+$ NK cells as well as CD127$^+$ ILCs in infant intestines. **c** SPADE tree of viable EP CD45$^+$lin$^-$ lymphocytes. CD127$^+$ ILCs (yellow outline), NK cells (red outline), including CD127$^-$NKp44$^+$CD103$^+$lin$^-$ cells (blue outline) within NK cell population. Expression of NKp44 is shown by color coding in relative intensity. Node sizes represent the size of populations. SPADE analysis was computed by using the same signature parameters as in Fig. 1 (infant samples $N = 4$, adult samples $N = 5$, target number of nodes: 200, down sampled events target: 30%). Median frequencies indicated by red lines. Error bars define interquartile ranges between 75th and 25th percentiles. Statistical comparisons are Mann-Whitney *U* comparisons (**a**) and Wilcoxon matched-pairs signed rank tests (**b**). Asterisks represent the following *p*-values: $^*p < 0.05$ and $^{***}p < 0.001$

lower (median 31%, IQR 27−34% $p < 0.001$). Next, we assessed whether increased frequencies of NKp44$^+$ NK cells in adult intestines were due to their selective expansion and observed that absolute numbers of epithelial NKp44$^+$ NK cells were not higher in adults than in infants (Fig. 7a). Absolute numbers of lamina propria-derived NKp44$^+$ NK cells were in fact higher in infant compared to adult intestines ($p = 0.01$). Thus, NKp44 expression identifies an NK cell subset persisting in intestines from infancy to adulthood. A heatmap analysis of investigated NK cell markers illustrated this further by identifying three clusters of infant intestinal lin$^-$ cells. The first cell cluster was defined by high expression of NKG2A, perforin, granzyme B, and Eomes, representing NK cells (Fig. 7b). A second cell cluster was identified by high expression of NKp44 and CD69, representing previously described ieILC1s[38]. The third cluster comprised CD127$^+$ ILCs. Intestinal CD127$^+$ ILCs were CD69$^+$ with low expression of CD103 and CD49a, in particular adult lamina propria-derived CD127$^+$ ILCs. Infant intestinal CD127$^+$ ILCs differed from NK cells, as only low frequencies of CD127$^+$ ILCs expressed either NKG2A or KIR (Supplementary Fig. 6). Eomes was detected in only 8% (median, IQR 1–12%) of infant and 12% (median, IQR 1–49%) of adult epithelial CD127$^+$ ILCs. Intestinal CD127$^+$ ILCs

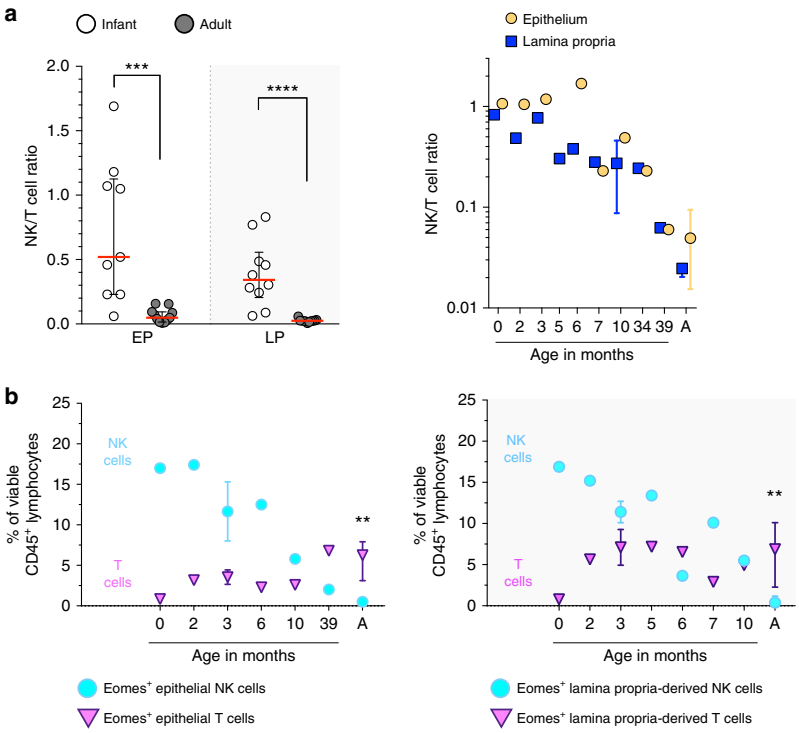

Fig. 8 Increase of intestinal Eomes$^+$ T cells in the first year of life. **a** NK-T cell ratios of infant (white circles) and adult intestines (dark circles, A) in epithelium (EP, yellow circles) and lamina propria (LP, blue squares) (infant EP samples ($N = 9$) and LP samples ($N = 10$), adult EP and LP samples ($N = 11$). **b** Frequencies of epithelium and lamina propria-derived Eomes$^+$ NK (turquoise circles) and Eomes$^+$ T cells (violet triangles) within the total lymphocyte pool at different ages (infant EP and LP samples ($N = 7$) and adult EP and LP samples ($N = 10$)). Median frequencies indicated by red lines. Error bars define interquartile ranges between 75th and 25th percentiles. Statistical comparisons are Mann-Whitney *U* comparisons. Asterisks represent the following *p*-values: $^{**}p < 0.01$; $^{***}p < 0.001$; and $^{****}p < 0.0001$

furthermore exhibited a non-cytotoxic phenotype, as perforin and granzyme B expressions were low in both infant and adult intestinal CD127$^+$ ILCs (Supplementary Fig. 6). NKp44 was expressed by 52% (median, IQR 44–66%) of infant and 50% (median, IQR 31–69%) of adult CD127$^+$ ILCs. The phenotype of CD127$^+$ ILCs more closely resembled the cluster of NKp44$^+$ CD69$^+$ NK cells in infant and adult intestines. Although functional responses of infant CD127$^+$ ILCs were relatively heterogeneous upon PMA and ionomycin stimulation, frequencies CD107a$^+$CD127$^+$ ILCs were relatively low, as was IFN-γ and TNF-α production (Supplementary Fig. 6). Taken together, innate lymphocyte populations in infant intestines consisted of a large population of prototypic CD127$^-$ NK cells and a smaller population of CD127$^+$ ILCs, which both declined during childhood, while a population of NKp44$^+$CD69$^+$ ieILC1s persisted.

To further illustrate dynamic changes of these ILC populations, we performed a spanning-tree progression analysis of density-normalized events (SPADE)[40] of multi-parameter flow cytometry data, based on CD16, CD56, CD127, CD7, KIR, CD94, NKp44, NKp46, NKp80, CD103, CD49a, and CD69 by viable CD45$^+$ lin$^-$ lymphocytes. SPADE allowed to determine phenotypic hierarchies of different populations of lin$^-$ lymphocytes in infant and adult intestines. The size of a respective circle indicates the size of the population, whereas distances between circles in the tree reveal phenotypic similarity of different populations. The SPADE tree showed that NK cells constituted the largest population of infant epithelial lin$^-$ lymphocytes (Fig. 7c). In contrast, in the SPADE tree of adult epithelial lin$^-$ lymphocytes, NKp44$^+$CD103$^+$ ieILC1s were most abundant. Together these results show that a population of intestinal NKp44$^+$lin$^-$ cells remained relatively stable over life; however, its contribution to the overall innate lymphocyte population in intestines increased over age due to a decrease of NKp44$^-$ NK cells during infancy.

NK cell decline coincides with Eomes$^+$ T cell accumulation. Infants are well-known for immaturity of their adaptive immune system, in particular cytotoxic CD8$^+$ T cells[41]. In line with this, we have previously shown that at birth the majority of intestinal T cells are CD4$^+$ T cells whereas cytotoxic CD8$^+$ T cells are scarce[42]. However, the CD4/CD8 T cell ratio changes over age, and in adults an abundance of epithelial CD103$^+$CD69$^+$Eomes$^+$ CD8$^+$ T cells has been shown to provide protection against intracellular pathogens[43,44]. We therefore examined ratios between NK cells and T cells in intestinal samples over age. Epithelial NK/T ratios rapidly declined from 0.52 (median, IQR 0.23–1.1) in infant intestines to 0.05 (median, IQR 0.02–0.09) in adult intestines ($p < 0.001$) (Fig. 8a). A similar trend was observed for NK/T cell ratios in intestinal lamina propria ($p < 0.001$) (Fig. 8a). These findings indicated a transition from an evenly balanced NK/T cell immune system in infant intestines to a T cell-dominated immune system in adult intestines. Frequencies of Eomes$^+$ T cells were determined to investigate whether a maturation of cytotoxic T cell responses coincided with changes in NK cell populations. At birth, intestinal epithelial and lamina propria-derived Eomes$^+$ T cells were rare. After birth,

Eomes$^+$ T cells increased, with highest frequencies of Eomes$^+$ T cells detected in adult intestines. Intestinal epithelial Eomes$^+$ T cells contributed 6% (median, IQR 3–8%) to the total epithelial lymphocyte population in adults and lamina propria-derived Eomes$^+$ T cells contributed 7% (median, IQR 2–10%) to the total lamina propria-derived lymphocyte population in adults (Fig. 8b). Taken together, the first year of life was characterized by rapid changes in intestinal NK cell and T cell compartments, with Eomes$^+$ NK cells declining and Eomes$^+$ T cells increasing.

Discussion

An increasing number of studies have shown that ILCs, including NK cells, are critical in host defense and can mediate tissue (re) modeling[6,8–10,12,13,38,45]. These studies primarily focused on fetal tissues or older children and adults[6,8–10,12,13,17,20,38,45]. However, studies investigating NK cells in infant intestines in the first year of life, when microbial colonization as well as rapid growth of mucosal tissues take place in concert, are lacking. Here, we demonstrate that NK cells represent the major innate lymphocyte population in small intestines of infants, whereas fewer NK cells persist in adult intestines. Infant intestinal NK cells demonstrated a strong effector phenotype characterized by Eomes, perforin, and granzyme B-expression compared to adult intestinal NK cells. NK cells decreased in infant intestines during the first year of life, concurring with an increase of Eomes$^+$ T cells. A population of NKp44$^+$CD103$^+$CD69$^+$ NK cells persisted in adult intestines, corresponding to previously described ieILC1s[38]. In conclusion, numerous prototypic NK cells populated small intestines in infancy and exhibited a cytotoxic effector profile, while adaptive immune responses were still immature.

Characterization of ILCs and NK cells is challenging in particularly in tissues due to lack of hallmark lineage markers for tissue-derived ILCs and NK cells[10,22–25]. Our analyses underlined the heterogeneity of ILCs and possible selection bias when for example only NKp80 or CD94 were included to identify NK cells. The well-documented plasticity of ILCs, varying origins of intestinal tissues included in previous studies and diverse pathologies may have further contributed to conflicting results reported on tissue-derived NK cells and ILCs[10,22–25,38,39]. Nonetheless, in general, non-cytotoxic ILCs are identified as CD127$^+$lin$^-$ cells, while NK cells are CD127$^-$Eomes$^+$lin$^-$ cells[10,46] and contain cytotoxic granules with perforin and granzyme B. Here we employed a comprehensive approach to characterize ILCs and developed a gating strategy that allowed to identify infant intestinal NK cells. Our findings show that a gating strategy based on CD56$^+$CD127$^-$lin$^-$ lymphocytes identified a large population of bona fide CD127$^-$Eomes$^+$ NK cells in infant intestines. Infant intestinal NK cells expressed integrin αE (CD103), indicating that these cells are prompted to remain tissue-resident[33]. In addition to NK cells, infant intestines contained CD127$^+$lin$^-$ ILC and NKp44$^+$CD69$^+$CD56$^+$CD127$^-$NK cell populations, which had lower Eomes and perforin expression. The NKp44$^+$CD69$^+$CD56$^+$CD127$^-$NK cell population persisted in adult intestines, as previously described[38]. Thus NK cells in infant intestines have a distinct phenotype compared to adult intestines.

Previous studies have described NK cells and non-cytotoxic ILCs in fetal tissues[16,17]. Although the role of ILCs as lymphoid tissue-inducers is well defined[47], the physiological role of intestinal NK cells prior to birth remains unknown. We detected the largest numbers of intestinal NK cells from birth to 6 months of age, suggesting that local NK cell populations are established early during human development. In line with previous data from fetal liver and lung tissues[48], infant intestinal NK cells had a relatively immature phenotype, but were equipped with cytolytic granules and had superior degranulation capacity compared to adult NK cells. The decrease of infant intestinal NK cell and CD127$^+$ ILC numbers coincided with an influx of Eomes$^+$ T cells in infant intestines. The intestinal epithelium of adults contains large numbers of tissue-resident CD8$^+$ T cells, which provide local antiviral immunity[43,49]. Our study shows that during human immune ontogeny, NK cells and CD127$^+$ ILCs preceded adaptive cytotoxic CD8$^+$ T cell responses. Infant intestinal NK cells were equipped with cytotoxic granules providing early innate effector responses, whilst CD8$^+$ T cell responses still developed. Changes occurring in intestinal lymphocyte populations in the first year of life are reminiscent of the contraction of the NK cell pool during viral infection, where NK cells constitute early antiviral responses followed by their rapid decrease upon induction of Eomes$^+$ CD8$^+$ T cells. A competitive disadvantage of NK cells compared to CD8$^+$ T cells for cytokines, such as IL-2 has been suggested as an underlying mechanism[50–53]. A similar developmental program appears to take place during immune ontogeny in infancy, suggesting a general pathway of immune constitution in different settings. Due to limitations in obtaining longitudinal human intestinal samples from birth to adulthood, the results presented here are derived from cross-sectional data. A causal sequence of events is therefore not possible. However, analyses of human intestines at different ages demonstrated a consistent pattern of maturation of the intestinal lymphocyte compartment. The exact mechanisms underlying dynamic modifications in the lymphocyte compartment in intestines, such as diet and maturation of the microbiome, need to be determined in future studies.

Our data further shows that the decline of infant intestinal NK cells and CD127$^+$ ILCs primarily affected NKp44$^-$ populations, whereas NKp44$^+$CD103$^+$CD69$^+$ NK cells persisted in adult intestines. NKp44$^+$CD103$^+$CD69$^+$ NK cells have been previously described in adult intestines and, although classified as ILC1s, share similarities with NK cells[38]. In the SPADE tree of adult epithelial lin$^-$ lymphocytes, CD127$^+$lin$^-$ cell populations and NKp44$^+$CD127$^-$NK cell/ieILC1 populations clustered closely together, indicating similarity. Future studies investigating these cell populations need to determine their hallmark cytokines. Next to a decline of NKp44$^-$ NK cells we furthermore observed a decrease of CD127$^+$ ILCs in infant intestines. This suggests that the decrease of infant intestinal NK cells was not due to ILC plasticity[17,25] or transition of CD127$^-$ NK cells into CD127$^+$ ILCs. As mentioned above, competition for cytokines is an important factor modulating the composition of lymphocyte populations in different anatomical locations[50–53]. Tissue-resident CD8$^+$ T cells also express CD127[44,54]. Thus, upon influx of CD8$^+$ T cells IL-2 and IL-7 are likely depleted, reducing survival signals for both NK cells and CD127$^+$ ILCs. In contrast NKp44$^+$CD103$^+$ ieILC1s seemed relatively resistant to this influx of CD8$^+$ T cells. Fuchs et al. showed that NKp44$^+$CD103$^+$ ieILC1s have a higher expression of CD122 (IL2-Rβ) compared to NKp44$^-$lin$^-$ lymphocytes and ILC3s, potentially allowing NKp44$^+$CD103$^+$ ieILC1s an enhanced usage of IL-2 for survival. Taking together, the first year of life is characterized by highly dynamic changes within intestinal lymphocyte populations.

In conclusion, our study demonstrates that intestinal NK cells represent the major cytotoxic lymphocyte population early in human intestinal development. During the first year of life intestinal NK cells as well as CD127$^+$ ILCs declined upon colonization of intestinal tissues with Eomes$^+$ T cells, with a population of NKp44$^+$CD103$^+$CD69$^+$ ieILC1s persisting in adult intestines. The first year of life is characterized by exposure to large numbers of microbes and changes in dietary intake. These factors have been shown in animal models to impact intestinal immune cell populations with repercussions for development of diseases later in life[55–58]. Our findings show that also in humans

significant modifications of innate lymphocyte populations take place during this dynamic phase of development, which may underlie specific pathologies observed in infancy.

Methods

Human tissue sample collection. Human tissues were collected after donors (adults) or their guardians (infants) provided written informed consent. Pediatric small intestinal tissues (median age 5.5 months, IQR 2.3–9.3, $N = 16$) were obtained upon surgery to correct gastrointestinal congenital abnormalities and reconstruction of ileostomy. Adult small intestinal samples (median age 57 years, IQR 42.3–65, $N = 13$) were collected upon ileostomy reconstructions. None of the donors suffered from inflammatory diseases. Tissues were obtained with approval of the ethics committee of the Medical Association of the Freie Hansestadt Hamburg (Ärztekammer Hamburg).

Lymphocyte isolation from human blood and intestinal tissues. Tissue and blood samples were transported at 4 °C and processed in the laboratory within 6 h after surgery. The mononuclear cell fraction was isolated from blood using a density gradient. Blood was diluted 1:1 with Hank's balanced salt solution (HBSS; Sigma-Aldrich), then layered on top of BIOCOLL (Biochrom GmbH) and centrifuged. The mononuclear cell fraction was aspirated and washed with phosphate buffered saline (PBS). Intestinal tissues obtained at surgery were first washed with PBS to remove feces and blood. The muscular layer was removed. The sizes of intestinal tissues were documented after removal of the muscular layer. Intestinal tissues were next cut into 0.5 × 0.5 cm segments and incubated for 2 × 20 min, at 37 °C with Iscove's modified Dulbecco's medium (IMDM; Thermo Fisher Scientific) supplemented with 5 mM ethylenediaminetetraacetic acid (EDTA; Sigma-Aldrich), 2 mM 1,4-dithiothreitol (DTT; Carl Roth GmbH+Co. KG) and 1% fetal bovine serum (FBS; Biochrom GmbH) to detach the epithelial layer. Supernatant was filtered through a 70 µm cell strainer to obtain a single cell solution. Epithelial lymphocytes were isolated by density gradient centrifugation using BIOCOLL (Biochrom GmbH). The remaining intestinal tissue was minced and digested for 2 × 30 min at 37 °C with IMDM (Thermo Fisher Scientific) supplemented with 1 mg/ml Collagenase D (Sigma-Aldrich), 1% FBS (Biochrom GmbH) and 1000 U/ml DNAse I (STEMCELL Technologies). Supernatant containing cells was filtered through a 70 µm strainer to obtain a single cell solution. Lamina propria lymphocytes were isolated from single cell suspensions using a Percoll gradient (VWR International); standard isotonic Percoll solution (SIP) was prepared by supplementing 100% Percoll with 10% 10X PBS, using an additional 1X PBS which resulted in 60% SIP solution. After isolation, the numbers of viable cells were counted using Trypan blue.

Flow cytometric analyses. Isolated lymphocytes from human infant and adult small intestines were analyzed using 18-parameter flow cytometry. For surface staining, cells were incubated in PBS with the appropriate monoclonal antibodies and Zombie Aqua™ for 30 min at 4 °C, washed and fixed with 1X stabilizing fixative (BD Biosciences).

The following monoclonal antibodies (all anti-human) were used for surface staining (clone, catalog number, dilution): CD3-BUV395 (UCHT1, 563546, 1:80), CD56-BV786 (NCAM16.2, 564058, 1:100), CD16-BUV737 (3G8, 564434, 1:80), CD57-BV605 (NK-1, 563895, 1:160) from BD Bioscience. CD45-BV711 (HI30, 304049, 1:100), CD45-Alexa Fluor 700 (2D1, 368514, 1:80), CD14-PE-Cy7 (M5E2, 301814, 1:100), CD14-BV510 (M5E2, 301842, 1:100), CD19-PE-Cy7 (SJ25C1, 363011, 1:100), CD19-BV510 (HIB19, 302242, 1:100), CD127-PE-Dazzle594 (A019D5, 351336, 1:100), CD103-PE-Cy7 (Ber-ACT8, 350212, 1:100), CD69-BV711 (FN50, 310944, 1:80), CD69-BV605 (FN50, 310938, 1:50), CD69-BV421 (FN50, 310930, 1:200), NKp46/CD335-BV421 (9E2, 331913, 1:40), NKp44/CD336-PE (P44-8, 352107, 1:40), CXCR6/CD186-PE-Cy7 (K041E5, 356012, 1:20), CD107a-BV421 (H4A3, 328626, 1:40) from BioLegend. CD103-PerCP-eFluor710 (Ber-ACT8, 46-1037-42, 1:40), CD7-APC-eFluor780 (eBio124-1D1, 47-0079-41, 1:80) from eBioscience. CD94-FITC (REA113, 130-098-975, 1:40), NKG2A/CD159a-APC (REA110, 130-098-809, 1:40), NKp44/CD336-PE-Vio770 (2.29, 130-104-195, 1:40), KIR2D/CD158a-PE (NKVFS1, 130-092-688, 1:160), KIR3DL1/DL2/CD158e/k-PE (REA970, 130-095-205, 1:80), CD49a-APC-Vio770 (TS2/7, 130-101-406, 1:40) from Miltenyi Biotec. hNKp80-APC (239127, FAB1900A, 1:40) from R&D Systems.

For intracellular staining, surface-stained cells were washed, then incubated with 1X Cytofix reagent (eBioscience), washed again and incubated with 1X Cytoperm reagent (eBioscience) and the appropriate monoclonal antibodies for 30 min at 4 °C. The following monoclonal antibodies were used for intracellular staining: T-bet-BV711 (4B10, 644819, 1:40), perforin-PerCP-Cy5.5 (d9G, 308114, 1:40), IFN-γ-FITC (B27, 506504, 1:40), TNF-α-BV605 (MAb11, 502936, 1:40), granzyme B-FITC (GB11, 515403, 1:40) from BioLegend. Eomes-eFluor 660 (WD1928, 50-4877-42, 1:40) from eBioscience. Zombie Aqua™ Fixable Viability Kit (BioLegend) was used to determine cell viability. Stained cells were analyzed using a BD LSRFortessa cell analyzer (BD Biosciences) within 24 h and data was analyzed using FlowJo software v10 (TreeStar, Ashland, Oregon, USA).

NK cell degranulation and cytokine production assay. Intestinal isolated monocuclear cells were resuspended in IMDM with 10% FBS, and either left unstimulated, stimulated with phorbol 12-myristate 13-acetate (PMA) (Sigma-Aldrich), and ionomycin (SantaCruz Biotechnology), K562 or 772.221 target cells (Effector/Target cell-ratio: 1:5), in the presence of Brefeldin A (Sigma Aldrich), Monensin (BD), and anti-CD107a-BV421 (BioLegend) for 6 h at 37 °C and 5% CO_2. The K562 cell line was obtained from the Leibniz institute DSMZ-German Collection of microorganisms and cell cultures. The 772.221 cell line was obtained from America Type Culture Collection (ATCC). Cells were intracellularly stained for cytokines and analyzed as described above. Values of response parameters (CD107a, IFN-ɣ, and TNF-α positive cells) from stimulated conditions were corrected with corresponding values of unstimulated conditions:

$$\text{Relative value} = \frac{\left(\text{percentage}_{\text{stim.cells}} - \text{percentage}_{\text{unstim.cells}}\right) * 100}{\left(100 - \text{percentage}_{\text{unstim.cells}}\right)}$$

Statistical analyses. The GraphPad Prism 7 (GraphPad Software, San Diego, CA) was used to analyze data and to perform statistical analyses. Statistical significance of differences was assessed using non-parametric Mann-Whitney U tests, or Wilcoxon matched-pairs signed rank test, for paired samples. Median frequencies and IQR are given in figures and text unless otherwise stated. Values of $p < 0.05$ were considered significant. NK cell populations were analyzed by dimensional reduction using Barnes–Hut t-distributed stochastic neighbor embedding (bht-SNE or viSNE) algorithm[26] and SPADE clustering[40] provided by the Cytobank platform (Cytobank Inc., Santa Clara, CA).

Data availability

Data used in this study have been collected in a clinical study and are subject to regulations of the Ethics Committee of the Ärztekammer Hamburg that approved these studies. Participant's written consent has been provided for data generation and handling according to approved protocols. Data storage is performed by the Heinrich Pette Institute. A Reporting Summary for this article is available as a Supplementary Information file. Data are available upon request from the corresponding author and can be shared after confirming that data will be used within the scope of the originally provided informed consent.

Received: 20 July 2018 Accepted: 18 December 2018
Published online: 28 February 2019

References

1. Yokoyama, W. M. & Plougastel, B. F. M. Immune functions encoded by the natural killer gene complex. *Nat. Rev. Immunol.* **3**, 304–316 (2003).
2. Moretta, L. & Moretta, A. Unravelling natural killer cell function: triggering and inhibitory human NK receptors. *EMBO J.* **23**, 255–259 (2004).
3. Vivier, E., Nunes, J. A. & Vely, F. Natural killer cell signaling pathways. *Science* **306**, 1517–1519 (2004).
4. Lanier, L. L. NK cell recognition. *Annu. Rev. Immunol.* **23**, 225–274 (2005).
5. Caligiuri, M. A. Human natural killer cells. *Blood* **112**, 461–469 (2008).
6. Klose, C. S. N. & Artis, D. Innate lymphoid cells as regulators of immunity, inflammation and tissue homeostasis. *Nat. Immunol.* **17**, 765–774 (2016).
7. Björkström, N. K., Ljunggren, H.-G. & Michaëlsson, J. Emerging insights into natural killer cells in human peripheral tissues. *Nat. Rev. Immunol.* **16**, 310–320 (2016).
8. Hanna, J. et al. Decidual NK cells regulate key developmental processes at the human fetal-maternal interface. *Nat. Med.* **12**, 1065 (2006).
9. Trowsdale, J. & Moffett, A. NK receptor interactions with MHC class I molecules in pregnancy. *Semin. Immunol.* **20**, 317–320 (2008).
10. Spits, H., Bernink, J. H. & Lanier, L. NK cells and type 1 innate lymphoid cells: partners in host defense. *Nat. Immunol.* **17**, 758–764 (2016).
11. Vivier, E. et al. Innate lymphoid cells: 10 years on. *Cell* **174**, 1054–1066 (2018).
12. Artis, D. & Spits, H. The biology of innate lymphoid cells. *Nature* **517**, 293–301 (2015).
13. Diefenbach, A., Colonna, M. & Romagnani, C. The ILC world revisited. *Immunity* **46**, 327–332 (2017).
14. Weizman, O.-E. et al. ILC1 confer early host protection at initial sites of viral infection. *Cell* **171**, 795–808.e12 (2017).
15. Phillips, J. H. et al. Ontogeny of human natural killer (NK) cells: fetal NK cells mediate cytolytic function and express cytoplasmic CD3 epsilon,delta proteins. *J. Exp. Med.* **175**, 1055–1066 (1992).
16. Ivarsson, M. A. et al. Differentiation and functional regulation of human fetal NK cells. *J. Clin. Invest.* **123**, 3889–3901 (2013).
17. Li, N. et al. Mass cytometry reveals innate lymphoid cell differentiation pathways in the human fetal intestine. *J. Exp. Med.* **215**, 1383–1396 (2018).

18. Sundström, Y. et al. The expression of human natural killer cell receptors in early life. *Scand. J. Immunol.* **66**, 335–344 (2007).
19. Dalle, J. H. et al. Characterization of cord blood natural killer cells: Implications for transplantation and neonatal infections. *Pediatr. Res.* **57**, 649–655 (2005).
20. Calleja, S. et al. Dynamics of non-conventional intraepithelial lymphocytes-NK, NKT, and gammadelta T-in celiac disease: relationship with age, diet, and histopathology. *Dig. Dis. Sci.* **56**, 2042–2049 (2011).
21. Fletcher, S. et al. Gastrointestinal pathogen distribution in symptomatic children in Sydney, Australia. *J. Epidemiol. Glob. Health* **3**, 11–21 (2013).
22. Simoni, Y. et al. Human innate lymphoid cell subsets possess tissue-type based heterogeneity in phenotype and frequency. *Immunity* **46**, 148–161 (2017).
23. Bernink, J. H., Mjösberg, J. & Spits, H. Human ILC1: to be or not to be. *Immunity* **46**, 756–757 (2017).
24. Bernink, J. H. et al. Human type 1 innate lymphoid cells accumulate in inflamed mucosal tissues. *Nat. Immunol.* **14**, 221–229 (2013).
25. Bernink, J. H. et al. Interleukin-12 and -23 control plasticity of CD127+ Group 1 and Group 3 innate lymphoid cells in the intestinal lamina propria graphical. *Immunity* **43**, 146–160 (2015).
26. Amir, E. A. D. et al. ViSNE enables visualization of high dimensional single-cell data and reveals phenotypic heterogeneity of leukemia. *Nat. Biotechnol.* **31**, 545–552 (2013).
27. Freud, A. G. et al. NKp80 defines a critical step during human natural killer cell development. *Cell Rep.* **16**, 379–391 (2016).
28. Kruse, P. H., Matta, J., Ugolini, S. & Vivier, E. Natural cytotoxicity receptors and their ligands. *Immunol. Cell Biol.* **92**, 221–229 (2014).
29. Mackay, L. K. et al. Cutting edge: CD69 interference with sphingosine-1-phosphate receptor function regulates peripheral T cell retention. *J. Immunol.* **194**, 2059–2063 (2015).
30. Hadley, G. A. & Higgins, J. M. G. Integrin alphaEbeta7: molecular features and functional significance in the immune system. *Adv. Exp. Med. Biol.* **819**, 97–110 (2014).
31. Cepek, K. L. et al. Adhesion between epithelial cells and T lymphocytes mediated by E-cadherin and the αEβ7 integrin. *Nature* **372**, 190 (1994).
32. Kramer, R. H. & Marks, N. Identification of integrin collagen receptors on human melanoma cells. *J. Biol. Chem.* **264**, 4684–4688 (1989).
33. Gasteiger, G., Fan, X., Dikiy, S., Lee, S. Y. & Rudensky, A. Y. Tissue residency of innate lymphoid cells in lymphoid and nonlymphoid organs. *Science* **350**, 981–985 (2015).
34. Lunemann, S. et al. Hobit expression by a subset of human liver-resident CD56bright Natural Killer cells. *Sci. Rep.* **7**, 6676 (2017).
35. Björkström, N. K. et al. Expression patterns of NKG2A, KIR, and CD57 define a process of CD56dim NK cell differentiation uncoupled from NK cell education. *Blood* **116**, 3853–3864 (2010).
36. Stegmann, K. A. et al. CXCR6 marks a novel subset of T-bet lo Eomes hi natural killer cells residing in human liver. *Sci. Rep.* **6**, 1–10 (2016).
37. Harmon, C. et al. Tissue-resident Eomeshi T-betlo CD56bright NK cells with reduced proinflammatory potential are enriched in the adult human liver. *Eur. J. Immunol.* **46**, 2111–2120 (2016).
38. Fuchs, A. et al. Intraepithelial type 1 innate lymphoid cells are a unique subset of IL-12- and IL-15-responsive IFN-γ-producing cells. *Immunity* **38**, 769–781 (2013).
39. Koues, O. I. et al. Distinct Gene Regulatory Pathways for Human Innate versus Adaptive Lymphoid Cells. Cell **165**, 1134–1146 (2016).
40. Qiu, P. et al. Analysis extracting a cellular hierarchy from high-dimensional cytometry data with SPADE. *Nat. Biotechnol.* **29**, 886–891 (2011).
41. Prendergast, A. J., Klenerman, P. & Goulder, P. J. R. The impact of differential antiviral immunity in children and adults. *Nat. Rev. Immunol.* **12**, 636–648 (2012).
42. Bunders, M. J. et al. Memory CD4+CCR5+T cells are abundantly present in the gut of newborn infants to facilitate mother-to-child transmission of HIV-1. *Blood* **120**, 4383–4390 (2012).
43. Gebhardt, T. & Mackay, L. K. Local immunity by tissue-resident CD8+ memory T cells. *Front. Immunol.* **3**, 1–12 (2012).
44. Thome, J. J. C. et al. Early-life compartmentalization of human T cell differentiation and regulatory function in mucosal and lymphoid tissues. *Nat. Med.* **22**, 1–7 (2016).
45. Björkström, N. K., Ljunggren, H. & Michaëlsson, J. Emerging insights into natural killer cells in human peripheral tissues. *Nat. Publ. Gr.* **16**, 310–320 (2016).
46. Spits, H. et al. Innate lymphoid cells-a proposal for uniform nomenclature. *Nat. Rev. Immunol.* **13**, 145–149 (2013).
47. Van De Pavert, S. A. et al. Maternal retinoids control type 3 innate lymphoid cells and set the offspring immunity. *Nature* **508**, 123–127 (2014).
48. Collins, A., Rothman, N., Liu, K. & Reiner, S. L. Eomesodermin and T-bet mark developmentally distinct human natural killer cells. *JCI Insight* **2**, e90063 (2017).
49. Cheroutre, H., Lambolez, F. & Mucida, D. The light and dark sides of intestinal intraepithelial lymphocytes. *Nat. Rev. Immunol.* **11**, 445–456 (2011).
50. Sitrin, J., Ring, A., Garcia, K. C., Benoist, C. & Mathis, D. Regulatory T cells control NK cells in an insulitic lesion by depriving them of IL-2. *J. Exp. Med.* **210**, 1153–1165 (2013).
51. Gasteiger, G. et al. IL-2–dependent tuning of NK cell sensitivity for target cells is controlled by regulatory T cells. *J. Exp. Med.* **210**, 1167–1178 (2013).
52. Alvarez, M. et al. Increased antitumor effects using IL-2 with anti-TGF-β reveals competition between mouse NK and CD8 T cells. *J. Immunol.* **193**, 1709–1716 (2014).
53. Coles, M. C. et al. Role of T and NK cells and IL7/IL7r interactions during neonatal maturation of lymph nodes. *Proc. Natl Acad. Sci. USA* **103**, 13457–13462 (2006).
54. Mackay, L. K. et al. Hobit and Blimp1 instruct a universal transcriptional program of tissue residency in lymphocytes. *Science* **352**, 459–463 (2016).
55. Ardeshir, A. et al. Breast-fed and bottle-fed infant rhesus macaques develop distinct gut microbiotas and immune systems. *Sci. Transl. Med.* **6**, 252ra120 (2014).
56. An, D. et al. Sphingolipids from a symbiotic microbe regulate homeostasis of host intestinal natural killer T cells. *Cell* **156**, 123–133 (2014).
57. Olszak, T. et al. Microbial exposure during early life has persistent effects on natural killer T cell function. *Science* **336**, 489–493 (2012).
58. Kim, K. S. et al. Dietary antigens limit mucosal immunity by inducing regulatory T cells in the small intestine. *Science* **351**, 858–863 (2016).

Acknowledgements

We would like to thank all donors and their parents for participation in this study. Further we thank the colleagues from the Department of Pediatric Surgery, as well as Department of General, Visceral, and Thoracic Surgery of the UKE (Hamburg) for the collection of intestinal tissues. This work was supported by the Deutsche Forschungsgemeinschaft (DFG) through the SFB841 and Daisy Huët Röell Foundation.

Author contributions

M.J.B. and A.F.S. designed the experiments. F.S. and R.R.C.E.S. contributed to experiments; D.P. and K.R. collected the tissue samples; S.L., C.K., and M.A. contributed to the study design, interpretation of the data, and manuscript revision; A.F.S. performed the data analyses. A.F.S. and M.J.B. wrote the manuscript with input from all authors. M.J.B. supervised the study.

Additional information

Supplementary Information accompanies this paper at https://doi.org/10.1038/s41467-018-08267-7.

Competing interests: The authors declare no competing interests.

Reprints and permission information is available online at http://npg.nature.com/reprintsandpermissions/

Journal peer review information: *Nature Communications* thanks the anonymous reviewers for their contribution to the peer review of this work. Peer reviewer reports are available.

Publisher's note: Springer Nature remains neutral with regard to jurisdictional claims in published maps and institutional affiliations.

Zusammenfassende Darstellung der Publikation mit Einordnung in den wissenschaftlichen Kontext

Einleitung

Natürliche Killerzellen (NK-Zellen) sind Lymphozyten des angeborenen Immunsystems, welche anders als jene des adaptiven Immunsystems nicht über antigenspezifische T- oder B- Zellrezeptoren verfügen (Lanier, 2005; Moretta & Moretta, 2004; Vivier, Nunes, & Vely, 2004; Yokoyama & Plougastel, 2003). In der aktuell verwendeten Nomenklatur werden NK-Zellen zu der Gruppe der Innate lymphoid cells (ILCs) gezählt (Krabbendam, Bernink, & Spits, 2021; Panda & Colonna, 2019; Spits et al., 2013; Spits, Bernink, & Lanier, 2016; Vivier et al., 2018) und spielen funktionell eine entscheidende Rolle unter anderem in der Verteidigung des Organismus aber auch beim Umbau und der Entwicklung verschiedener Gewebe (Björkström, Ljunggren, & Michaëlsson, 2016; H. Fan et al., 2019; Hanna et al., 2006; Klose & Artis, 2016; Tang, Xu, & Jin, 2020; Trowsdale & Moffett, 2008). Innerhalb der heterogenen Gruppe der Innate lymphoid cells wird weiterhin unter anderem in klassische ILCs und NK-Zellen unterschieden. Klassische ILCs werden gemeinhin über die Expression der IL-7 Rezeptor-α-Kette (CD127) identifiziert, und häufig als das Gegenstück zu T-Helferzellen im angeborenen Immunsystem angesehen (ILC1s, ILC2s und ILC3s) (Artis & Spits, 2015; Diefenbach, Colonna, & Romagnani, 2017; Krabbendam et al., 2021). NK-Zellen hingegen werden als $CD127^-$ klassifiziert und weisen dabei im Allgemeinen ein höheres zytotoxisches Potential als andere ILCs auf (Spits et al., 2016; Vivier et al., 2018). Diese Zytotoxizität wird neben anderen Mechanismen vor allem über die Sekretion von zytotoxischen Granula vermittelt, was es NK-Zellen ermöglicht entartete oder virus-infizierte Zellen zu eliminieren (Caligiuri, 2008). Sowohl NK-Zellen als auch ILC1s besitzen zudem die Fähigkeit pro-inflammatorische Zytokine wie etwa Tumornekrosefaktor-α (TNF-α) und Interferon-ɣ (IFN-γ) zu produzieren (Spits et al., 2016; Vivier et al., 2018). Darüber hinaus zeigen sich auch ILCs im Allgemeinen, in verschiedenen Geweben in der Lage lokale Immunantworten gegenüber Infektionen zu vermitteln (Klose & Artis, 2016; Weizman et al., 2017) und sind bereits früh in der Entwicklung des menschlichen Organismus nachweisbar. So wurden ILCs und NK-Zellen bisweilen auch in fetaler Darmmukosa beschrieben (Ivarsson et al., 2013; Li et al., 2018; Phillips et al., 1992). Allerdings

basierte bislang das meiste Wissen über die Entwicklung des *kindlichen* NK-Zellkompartiments auf Studien aus Nabelschnurblut oder Geweben von älteren Kindern (Calleja et al., 2011; Dalle et al., 2005; Sundström et al., 2007). Dies scheint in erster Linie den Schwierigkeiten, die eine Probenakquirierung von Neugeborenen und Kleinkindern mit sich bringt, geschuldet (Sagebiel et al., 2019). Die genaue Zusammenstellung des intestinalen angeborenen Immunsystems, sowie deren Dynamiken im ersten Lebensjahr blieben daher bis dato unklar. Das erste Lebensjahr ist hierbei von besonderem Interesse, da Neugeborene in dieser Entwicklungsphase das erste Mal mit Antigenen aus Nahrung und Umwelt in Kontakt treten, die bakterielle Kolonisation des Darmes stattfindet und Säuglinge insbesondere in dieser Zeit eine hohe Empfänglichkeit gegenüber viralen Infektionen aufweisen (Fletcher et al., 2013; Sagebiel et al., 2019). In dieser Publikation konnte gezeigt werden, dass NK-Zellen die größte Lymphozytenpopulation des angeborenen Immunsystems im Dünndarm von Neugeborenen darstellen und bereits eine große funktionelle Potenz, vermittelt durch Perforin- und Granzym B-beinhaltende Granula aufweisen (Sagebiel et al., 2019). Gewebeproben von erwachsenen Probanden enthielten im Gegensatz dazu nur wenig NK-Zellen in der Dünndarmmukosa (Sagebiel et al., 2019).

Ergebnisse

Im Folgenden erfolgt eine zusammenfassende Darstellung der Ergebnisse. Bezüglich der detaillierten Daten und Abbildungen wird hierbei auf die oben eingefügte Originalarbeit verwiesen (Sagebiel et al., 2019).

Basierend auf in der Literatur beschriebener Oberflächenmoleküle zur Charakterisierung und Identifikation von NK-Zellen (CD16, CD56, CD127, CD7, KIR, CD94, NKp44, NKp46, NKp80, CD103, CD49a, und CD69) wurden zunächst detaillierte durchflusszytometrische Analysen von lebenden Lymphozyten aus Epithel, Lamina propria und peripherem Blut durchgeführt (Sagebiel et al., 2019). Mithilfe von Dimensionsreduktion mittels des viSNE-Algorithmus konnte daraufhin eine Gating-Strategie ($CD127^{-}CD56^{+}CD45^{+}lin^{-}$) für intestinale NK-Zellen etabliert werden (Sagebiel et al., 2019). Auf Grundlage dieser Gating-Strategie erfolgte zunächst die Quantifizierung intestinaler NK-Zellen bei Neugeborenen und Erwachsenen sowie die Erhebung der absoluten Zellzahl/cm^2 Mukosa. Hierbei ergaben sich deutlich höhere Werte sowohl im prozentualen Anteil als auch bei den absoluten Zellzahlen bei

Neugeborenen (Sagebiel et al., 2019). Es erfolgte zudem die weitergehende Charakterisierung intestinaler NK-Zellen bei Neugeborenen und Erwachsenen. Intestinale NK-Zellen zeigen sich phänotypisch als gewebeansässig (*tissue-resident*), was durch eine hohe Expression von CD103, CD49a sowie CD69 abgebildet wird (Sagebiel et al., 2019). Bei Neugeborenen waren intestinale NK-Zellen durch einen eindeutigen Effektor-Phänotyp gekennzeichnet, welcher durch eine hohe Eomes-, Perforin-, und Granzym B-Expression charakterisiert war. Dies zeigte sich insbesondere im Vergleich zu intestinalen NK-Zellen von Erwachsenen (Sagebiel et al., 2019). Auch in funktionellen Experimenten konnte bei intestinalen NK-Zellen von Neugeborenen eine stärkere Degranulation nach Stimulation, als bei jenen von erwachsenen Probanden detektiert werden (Sagebiel et al., 2019). Sowohl die absolute als auch die relative Anzahl intestinaler NK-Zellen präsentierte sich im ersten Lebensjahr deutlich rückläufig, begleitet von einem Zuwachs an $Eomes^+$ T-Zellen (Sagebiel et al., 2019). Eine Subpopulation von $NKp44^+CD103^+CD69^+$NK-Zellen/ILCs persistierte zudem in der Dünndarmmukosa von Erwachsenen, analog zu den zuvor beschriebenen ieILC1s (Fuchs et al., 2013; Sagebiel et al., 2019).

Diskussion

Identifikation von NK-Zellen in intestinalen Geweben

Um vergleich- und reproduzierbare Analysen spezifischer Populationen von Lymphozyten durchzuführen bedarf es einer einheitlichen Nomenklatur. Das Fehlen von eindeutig etablierten Lineage-Markern zur Identifizierung Gewebe-entstammender ILCs und NK-Zellen stellt in diesem Zusammenhang eine besondere Herausforderung dar (Bernink et al., 2015; Bernink, Mjösberg, & Spits, 2017; Bernink et al., 2013; Dogra et al., 2020; Simoni et al., 2017; Spits et al., 2016). Daher erfolgte zunächst die oben beschriebe detaillierte Analyse verschiedener in der Literatur zu findender Lineage-Marker auf Lymphozyten aus Epithel, Lamina propria und peripherem Blut (Sagebiel et al., 2019). In den durchgeführten viSNE-Analysen bestätig sich die Heterogenität der verschiedenen ILC-Populationen im Gewebe, vor dessen Hintergrund sich weiterhin ein möglicher Selektionsbias vermuten lässt, wenn lediglich einzelne Markermoleküle wie etwa NKp80 oder CD94 zur Identifikation von NK-Zellen verwendet werden (Sagebiel et al., 2019). Die Plastizität von ILCs, unterschiedliche Ursprungsgewebe und variierende Pathologien in vorangegangenen Studien könnten

zudem weiter zu widersprüchlichen Ergebnissen bezüglich gewebeansässigen NK-Zellen und ILCs beigetragen haben (Bernink et al., 2015, 2017, 2013; Dogra et al., 2020; Fuchs et al., 2013; Koues et al., 2016; Sagebiel et al., 2019; Simoni et al., 2017; Spits et al., 2016). Nichtsdestotrotz werden im Allgemeinen nicht-zytotoxische ILCs als $CD127^{+}lin^{-}$ Zellen definiert (Krabbendam et al., 2021; Spits et al., 2013, 2016; Vivier et al., 2018), wohingegen NK-Zellen als $CD127^{-}Eomes^{+}lin^{-}$ Zellen (Krabbendam et al., 2021; Spits et al., 2013, 2016) gelten und zudem zytotoxischen Granula mit Perforin und Granzym B enthalten (Sagebiel et al., 2019; Spits et al., 2013, 2016).
Auf dieser Grundlage konnte eine Gating-Strategie entwickelt werden, um intestinale NK-Zellen bei Neugeborenen zu identifizieren. Die Analysen zeigen, dass eine Gating-Strategie basierend auf $CD56^{+}CD127^{-}lin^{-}$ Lymphozyten eine große Population tatsächlicher $CD127^{-}Eomes^{+}$ NK-Zellen im Neugeborenendünndarm identifiziert (Sagebiel et al., 2019).

Potentielle Funktionen von NK-Zellen im Darm von Neugeborenen

Jene intestinale NK-Zellen, sowohl von Neugeborenen als auch von Erwachsenen zeigen sich phänotypisch als gewebeansässig (*tissue-resident*) (Sagebiel et al., 2019). *Tissue-residency* beschreibt hierbei das immunologisches Konzept, dass verschiedene anatomische Kompartimente, spezifische und klar differenzierbare Lymphozytenpopulationen mit dezidierten Phänotypen, Funktionen und gegebenenfalls auch separater Entwicklung aufweisen (Cepek et al., 1994; Gasteiger, Fan, Dikiy, Lee, & Rudensky, 2015; Hadley & Higgins, 2014; Kramer & Marks, 1989; Mackay et al., 2015). Dem Einfluss tissue-residenter/gewebeansässiger Lymphozyten wird zuletzt in verschiedenen Geweben und Organen eine besondere Bedeutung beigemessen (Björkström et al., 2016; Dogra et al., 2020; Fan & Rudensky, 2016; Gebhardt & Mackay, 2012; Hess et al., 2020; Martrus et al., 2019; Stegmann et al., 2016). Darüber hinaus enthielt die Dünndarmmukosa von Neugeborenen $CD127^{+}lin^{-}$ ILC- und $NKp44^{+}CD69^{+}CD56^{+}CD127^{-}$ NK-Zellpopulationen mit einer niedrigeren Eomes- und Perforin-Expression (Sagebiel et al., 2019). Jene $NKp44^{+}CD69^{+}CD56^{+}CD127^{-}$ NK-Zellpopulation persistierte im Dünndarm von Erwachsenen (Sagebiel et al., 2019), wie zuvor im Sinne von ieILCs beschrieben (Fuchs et al., 2013). Diesbezüglich lässt sich festhalten, dass intestinale NK-Zellen bei Neugeborenen einen deutlich abweichenden Phänotyp verglichen mit ieILCs von Erwachsenen aufweisen (Sagebiel et al., 2019).

NK-Zellen und nicht-zytotoxische ILCs wurden bereits in vorherigen Arbeiten in fetalem Gewebe nachgewiesen (Ivarsson et al., 2013; Li et al., 2018). Hierbei zeigt sich jedoch insbesondere die physiologische Rolle intestinaler NK-Zellen pränatal weiter unklar. Die höchsten Zahlen jener intestinalen NK-Zellen konnten in den ersten sechs Lebensmonaten nachgewiesen werden, was nahelegt, dass lokale NK-Zellpopulationen bereits früh während der menschlichen Entwicklung angelegt werden (Sagebiel et al., 2019). Die Populationen wiesen dabei einen relativ unreifen Phänotyp auf, was sich mit Ergebnissen anderer Arbeitsgruppen, die fetales Leber- und Lungengewebe untersuchten deckt (Collins, Rothman, Liu, & Reiner, 2017). Trotz des unreifen Phänotyps sind intestinale NK-Zellen von Neugeborenen jedoch bereits mit zytolytischen Granula ausgerüstet und weisen funktionell eine erhöhte Degranulationskapazität verglichen mit Erwachsenen auf (Sagebiel et al., 2019). Zudem zeigten intestinale NK-Zellen von Neugeborenen bereits eine deutliche TNF-α- und IFN-ɣ-Sekretion (Sagebiel et al., 2019).

Vor diesem Hintergrund konnten wir in einer weiteren Publikation zeigen, dass $CD4^+$ T-Zellen als Vertreter des adaptiven Immunsystems TNF-α-vermittelt die Entwicklung der intestinalen Mukosa bereits pränatal beeinflussen. Hierbei stellt sich ein empfindliches Gleichgewicht dar, welches abhängig von der TNF-α-Sekretion zwischen Förderung der intestinalen Mukosaentwicklung und gewebezerstörender Inflammation schwankt (Schreurs et al., 2019). Letzteres Szenario kann dabei als weiterer Aspekt eines multifaktoriellen Erklärungsmodells für die Nekrotisierende Enterokolitis (NEC) bei Frühgeborenen verstanden werden (Schreurs et al., 2019). Allerdings sind hier grundlegenden Unterschiede in der Aktivierung von NK-Zellen und $CD8^+$ T-Zellen zu beachten. Während NK-Zellen vor allem durch die Erkennung von exprimierten Stressliganden und fehlenden MHC-I-Molekülen (*Missing-self-Hypothese*) von entarteten oder virus-infizierten Zellen aktiviert werden (French & Yokoyama, 2003; Trowsdale & Moffett, 2008; Yokoyama & Plougastel, 2003), erfolgt die Aktivierung $CD8^+$ T-Zellen über Bindung antigenspezifischer T-Zellrezeptoren im Zusammenspiel mit weiteren co-stimulatorischen Signalen (Janssen et al., 2003). Inwieweit die nachgewiesene TNF-α-Produktion der hier beschriebenen intestinalen NK-Zellen einen ähnlichen Einfluss auf jenes Gleichgewicht zwischen Wachstum und Inflammation ausübt, wie für T-Zellen bereits gezeigt (Schreurs et al., 2019), gilt es in künftigen Studien zu untersuchen. So kann im weiteren Verlauf folglich auch die Rolle

der zahlreichen gewebeansässigen NK-Zellen bei frühkindlichen intestinalen Pathologien wie etwa der NEC beurteilt werden.

Reduktion intestinaler NK-Zellen begleitet von einer Erhöhung $CD8^+$ T-Zellen

Der Rückgang von intestinalen NK-Zellen und $CD127^+$ILCs wird von einem Zuwachs an $Eomes^+$ T-Zellen in der Dünndarmmukosa begleitet (Sagebiel et al., 2019). Weiterhin sind im intestinalen Epithel von Erwachsenen eine große Zahl an gewebeansässigen $CD8^+$ T-Zellen, die eine lokale antivirale Immunität gewährleisten können, beschrieben (Cheroutre, Lambolez, & Mucida, 2011; Gebhardt & Mackay, 2012). Darüber hinaus konnten wir zuletzt $CD8^+$ T-Zellen nach Antigenexposition postnatal in intestinalen Proben von Neugeborenen nachweisen (Schreurs et al., 2020). Allerdings zeigten diese intestinalen $CD8^+$ T-Zellen wenig zytotoxische Granula und lediglich eine geringe Produktion an pro-inflammatorischen Zytokinen wie TNF-α und IFN-γ (Schreurs et al., 2020). Vor diesem Hintergrund scheint der beobachtete Rückgang von zytotoxischen NK-Zellen im ersten Lebensjahr funktionell zunächst nicht ausreichend durch $CD8^+$ T-Zellen kompensiert, was Kleinkinder potentiell in einer vulnerablen Phase im Kampf gegenüber viralen Infektionen zurücklassen könnte. Inwieweit $CD8^+$ T-Zellen in der weiteren Entwicklung an Zytotoxizität gewinnen und so gegebenenfalls eine ausreichende antivirale Immunität beim Erwachsenen gewährleisten können, gilt es in weiteren Experimenten zu untersuchen. Unsere Daten zeigen diesbezüglich vorerst, dass während der Entwicklung des intestinalen Immunsystems beim Menschen NK-Zellen und $CD127^+$ ILCs adaptiven $CD8^+$ T-Zell-Populationen vorausgehen (Sagebiel et al., 2019).

Die beschriebenen Veränderungen in intestinalen Lymphozytenpopulationen im ersten Lebensjahr erinnern hierbei an den Rückgang von NK-Zellpopulationen während einer viralen Infektion, wobei NK-Zellen die erste antivirale Immunantwort vermitteln, gefolgt von deren raschem Rückgang nach Induktion $Eomes^+CD8^+$ T-Zellen. Als zugrundeliegender Mechanismus für diese Dynamik wurde ein kompetitiver Nachteil von NK-Zellen gegenüber $CD8^+$ T-Zellen für Zytokine wie etwa IL-2 vermutet (Alvarez et al., 2014; Coles et al., 2006; Gasteiger et al., 2013; Sagebiel et al., 2019; Sitrin, Ring, Garcia, Benoist, & Mathis, 2013). Im Rahmen der individuellen menschlichen Entwicklung könnte ein äquivalenter Ablauf während der Kindheit stattfinden, im Sinne eines grundlegenden Mechanismus‘ der Immunregulation in verschiedenen Situationen (Sagebiel et al., 2019).

Bei den hier präsentierten Daten handelt es sich um Querschnittsdaten ohne longitudinale Beobachtungskomponente. Eine kausale Analyse der beobachteten Dynamiken ist daher nicht sicher möglich. Allerdings zeigen Untersuchungen von humanen Darmproben aus verschiedenen Altersgruppen ein konsistentes Muster der Reifung des intestinalen Immunkompartiments (Sagebiel et al., 2019). Die genauen Einflussfaktoren, denen die dynamischen Modifikationen im intestinalen Lymphozytenkompartiment unterliegen, wie etwa Ernährung (Ardeshir et al., 2014), Reifung des Mikrobioms (An et al., 2014; Olszak et al., 2012), oder intestinale Pathologien (Bernink et al., 2013; Poggi et al., 2019) sollten in künftigen Studien weiter adressiert werden (Sagebiel et al., 2019).

NKp44$^+$CD103$^+$CD69$^+$ Zellen persistieren im Sinne von ieILC1s

Die präsentierten Daten zeigen darüber hinaus, dass der Rückgang von intestinalen NK-Zellen und CD127$^+$ ILCs bei Kindern vor allem die NKp44$^-$ Populationen betrifft. In der Mukosa erwachsener Probanden scheinen hingegen vor allem NKp44$^+$CD103$^+$CD69$^+$ NK-Zellen zu persistierten (Sagebiel et al., 2019). In vorherigen Arbeiten als Subgruppe von ILC1s klassifiziert, wurden NKp44$^+$CD103$^+$CD69$^+$ NK-Zellen bereits in der Darmmukosa von Erwachsenen beschrieben (Fuchs et al., 2013). Trotz der in dieser Studie abweichenden Nomenklatur im Sinne von *intra-epithelialen ILC1 (ieILC1),* zeigen die beschriebenen Populationen einige Gemeinsamkeiten mit NK-Zellen (Fuchs et al., 2013; Krabbendam et al., 2021; Sagebiel et al., 2019).

Es existieren mittlerweile weitere Publikationen bezüglich solch intermediärer Populationen in diversen Geweben (Cella et al., 2019; Dogra et al., 2020) und peripherem Blut (Salomé et al., 2019), wobei hier die Nomenklatur mit der Einführung *zytotoxischer ILCs* (Krabbendam et al., 2021) bisweilen immer komplexer wird. Dieser Umstand könnte so die oft angestrebte Kategorisierung in klar definierte Populationen infrage stellen. Je genauer die Betrachtung, desto unschärfer erscheint teilweise die Abgrenzung etwa zwischen NK-Zellen und zytotoxischen ILCs (Krabbendam et al., 2021), oder zwischen ILC1 und ILC3 (Cella et al., 2019). Alternativ scheint ein mehr deskriptiver Ansatz der stattfindenden Dynamiken oder funktionellen Zusammenhänge, unter Berücksichtigung des Ursprungsgewebes und gegebenenfalls der zugrundeliegenden Pathologie sinnvoll, um das ILC-Spektrum adäquat abbilden und verstehen zu können.

Neben dem Rückgang von NKp44⁻ NK-Zellen konnte weiterhin auch einen Rückgang von CD127⁺ ILCs in der Darmschleimhaut von Kindern beobachtet werden (Sagebiel et al., 2019). Dies lässt die Annahme zu, dass der Rückgang von intestinalen NK-Zellen bei Neugeborenen nicht durch eine Transformation von CD127⁻ NK-Zellen in CD127⁺ ILCs zu erklären ist, und sich somit das in der Literatur beschriebene Konzept von ILC-Plastizität (Bernink et al., 2015; Li et al., 2018) hier nicht als Erklärung für die beschrieben Dynamiken eignet. Stattdessen kann ein Wettbewerb um proliferativ wirkende Zytokine zwischen den verschiedenen Lymphozytenpopulationen als geeigneteres Modell vermutet werden. Dies könnte den Rückgang von NK-Zellen und CD127⁺ ILCs auf der einen Seite und den Zuwachs an CD8⁺ T-Zellen auf der anderen Seite zu erklären (Alvarez et al., 2014; Coles et al., 2006; Gasteiger et al., 2013; Sagebiel et al., 2019; Sitrin et al., 2013). Gewebeansässige CD8⁺ T-Zellen exprimieren ebenfalls CD127 (Mackay et al., 2016; Thome et al., 2016). Daher könnte es durch ein vermehrtes Auftreten von CD8⁺ T-Zellen zu einem erhöhten Verbrauch von IL-2 und IL-7 kommen, was wiederum die Proliferations- und Überlebenssignale sowohl für NK-Zellen als auch CD127⁺ ILCs reduzieren könnte (Sagebiel et al., 2019).
Im Gegensatz dazu schienen NKp44⁺CD103⁺ ieILC1s relativ unbeeinträchtigt gegenüber dem Auftreten von CD8⁺ T-Zellen, da sie auch bei Erwachsenen konstant nachweisbar sind (Sagebiel et al., 2019). Fuchs et al. konnten zeigen, dass die hier als analog betrachteten NKp44⁺CD103⁺ ieILC1s eine höhere Expression von CD122 (Teil der β-Untereinheit des IL-2-Rezeptors) verglichen mit NKp44⁻lin⁻ Lymphozyten und ILC3s aufweisen (Fuchs et al., 2013). Dieser Umstand könnte NKp44⁺CD103⁺ ieILC1s eine effizientere Nutzung von IL-2 als Überlebenssignal ermöglichen (Sagebiel et al., 2019) und somit in dem skizzierten Wettbewerbsmodell dafür sorgen, dass jene Population bis ins Erwachsenenalter persistiert, während zytotoxische NK-Zellen dezimiert werden. Um diese Hypothesen weitergehend zu untersuchen bedarf es dezidierter Folgeexperimente mit Zytokin-Kompetitions-Assays der beschriebenen Populationen.

Fazit

Zusammengefasst zeigt sich das erste Lebensjahr durch hochdynamische Veränderungen im intestinalen Lymphozytenkompartiment von Säuglingen charakterisiert. Das erste Lebensjahr ist weiterhin durch eine Exposition gegenüber einer Vielzahl an Bakterien und Viren sowie durch eine drastische Veränderung der

enteralen Ernährung charakterisiert. Diese Faktoren konnten im Tiermodell als einflussreich auf intestinale Immunzellpopulationen gezeigt werden, mit weitreichenden Auswirkungen auch auf die Entwicklung späterer Pathologien (An et al., 2014; Ardeshir et al., 2014; Kim et al., 2016; Olszak et al., 2012). Insbesondere der Rückgang von zytotoxischen NK-Zellen in der Darmschleimhaut von Neugeborenen im ersten Lebensjahr, welcher durch $CD8^+$ T-Zellen zunächst lediglich teilkompensiert erscheint, kann in dieser kritischen Entwicklungsphase Kleinkinder einer erhöhten Vulnerabilität gegenüber viralen Infektionen aussetzen. Es zeigt sich, dass beim Menschen signifikante Modifikationen des angeborenen intestinalen Immunsystems bereits früh in der Entwicklung stattfinden, welche unter Umständen weitreichende Auswirkung auf spezifische immunologische und inflammatorische Krankheitsbilder in der Kindheit haben können.

Material und Methoden

Akquirierung humaner Darmproben

Die humanen Darmproben wurden nach Aufklärung und Einholung des schriftlichen Einverständnisses der Spender und/oder deren Eltern akquiriert. Dünndarmproben von Neugeborenen und Kindern (Medianes Alter 5.5 Monate, IQR 2.3–9.3, N=16) wurden im Rahmen der chirurgischen Korrektur angeborener gastrointestinaler Fehlbildungen sowie bei Ileostomarückverlagerungen gewonnen. Dünndarmproben von erwachsenen Probanden (Medianes Alter 57 Jahre, IQR 42.3–65, N=13) wurden ausschließlich im Rahmen von Ileostomarückverlagerungen gesammelt. Keiner der eingeschlossenen Probanden wies eine entzündliche Darmerkrankung auf. Die Probenakquirierung und Durchführung der Studie erfolgte mit Genehmigung des Ethikkomitees der Ärztekammer der Freien und Hansestadt Hamburg.

Lymphozytenisolation aus Blut und Darmmukosa

Blut- und Gewebeproben wurden bei 4°C transportiert und innerhalb von maximal sechs Stunden nach Probenentnahme prozessiert. Die Isolation der mononukleären Zellfraktion aus peripherem Blut erfolgte mittels Dichtegradientenzentrifugation. Hierfür wurde das Blut 1:1 mit *Hank's balanced salt solution* (HBSS; Sigma-Aldrich) verdünnt und daraufhin als eigene Phase auf *BIOCOLL* (Biochrom GmbH) aufgetragen. Anschließend folgte die Zentrifugation. Nach Zentrifugation wurde die

mononukleäre Zellfraktion mittels Pipette aspiriert und mehrfach mit *Phosphate buffered saline (PBS)* gewaschen.

Präparate intestinaler Gewebe, die während Operationen anfielen, wurden zunächst ausgiebig mit *PBS* gespült. Daraufhin erfolgte die scharfe Dissektion der intestinalen Muskelschicht. Die Oberfläche intestinaler Gewebestücke wurde nach Entfernung der Muskelschicht vermessen. Als nächstes erfolgte die Zerkleinerung der Mukosa in 0.5 × 0.5 cm Fragmente, welche dann für 2 × 20 Minuten, bei 37°C mit *Iscove's modified Dulbecco's medium* (*IMDM*; Thermo Fisher Scientific) versetzt mit 5 mM *Ethylenediaminetetraacetic acid* (*EDTA*; Sigma-Aldrich), sowie 2 mM *1,4-dithiothreitol* (*DTT*; Carl Roth GmbH & Co. KG) und 1% *fetalbovine serum* (*FBS*; Biochrom GmbH) unter leichter Vibration inkubiert wurden. In diesem Inkubationsschritt erfolgt die chemisch-mechanische Ablösung der Lamina epithelialis mucosae. Nach Inkubation wurde der Überstand durch einen 70 µm Zellfilter gespült, um eine Einzelzelllösung zu erhalten. Im nächsten Schritt wurden die epithelialen Lymphozyten aus dieser Lösung ebenfalls durch Dichtegradientenzentrifugation mittels *BIOCOLL* (Biochrom GmbH) isoliert. Das verbleibende Darmgewebe wurde daraufhin püriert und für 2 × 30 Minuten bei 37°C mit *IMDM* (Thermo Fisher Scientific), versetzt mit 1 mg/ml *Collagenase D* (Sigma-Aldrich), 1% *FBS* (Biochrom GmbH) und 1000 U/ml *DNAse I* (STEMCELL Technologies) weiter verdaut. In diesem Schritt erfolgte die enzymatische Verdauung der Lamina propria und somit die Freisetzung der dort enthaltenen Lymphozyten. Der zellhaltige Überstand wurde ebenfalls durch einen 70 µm Filter gewaschen, um so erneut eine Einzelzelllösung zu erhalten. Die Lamina propria-Lymphozyten wurden aus dieser Einzelzelllösung mittels Zentrifugation über einen *Percoll*-Gradienten (VWR International) isoliert. Hierfür wurde *Standard isotonic Percoll Lösung* (*SIP*) benutzt indem 100% *Percoll* mit 10% 10X *PBS* und zusätzlich 1X *PBS* versetzt wurde. Dies resultierte so in einer 60% *SIP*-Lösung. Nach Isolation wurden lebende Zellen unter dem Mikroskop mittels *Tryptan-Blau*-Färbung gezählt (Sagebiel et al., 2019). Die detaillierten Protokolle zur Lymphozytenisolation aus intestinalen Gewebeproben sind einer separaten Publikation unserer Arbeitsgruppe zu entnehmen (Schreurs et al., 2017)

Durchflusszytometrische Analysen

Die wie oben beschrieben isolierten Lymphozyten wurden mittels 18-Parameter-Durchflusszytometrie analysiert. Für die Oberflächenfärbung erfolgte die Inkubation in

PBS mit den entsprechenden monoklonalen Antikörpern sowie *Zombie Aqua*™ als Marker für tote Zellen. Die Inkubationszeit betrug 30 Minuten bei 4°C. Hierauf folgte die Waschung und Fixierung der Färbung mit 1X *Fixierungspuffer* (BD Biosciences). Die folgenden monoklonalen Antikörper (alle anti-human) wurden für die Oberflächenfärbung verwendet (Klon, Katalognummer, Verdünnung): *CD3-BUV395 (UCHT1, 563546, 1:80), CD56-BV786 (NCAM16.2, 564058, 1:100), CD16-BUV737 (3G8, 564434, 1:80), CD57-BV605 (NK-1, 563895, 1:160)* von BD Bioscience. *CD45-BV711 (HI30,304049, 1:100), CD45-Alexa Fluor 700 (2D1, 368514, 1:80), CD14-PE-Cy7 (M5E2,301814, 1:100), CD14-BV510 (M5E2, 301842, 1:100), CD19-PE-Cy7 (SJ25C1,363011, 1:100), CD19-BV510 (HIB19, 302242, 1:100), CD127-PE-Dazzle594 (A019D5, 351336, 1:100), CD103-PE-Cy7 (Ber-ACT8, 350212, 1:100), CD69-BV711 (FN50, 310944, 1:80), CD69-BV605 (FN50, 310938, 1:50), CD69-BV421 (FN50, 310930, 1:200), NKp46/CD335-BV421 (9E2, 331913, 1:40), NKp44/CD336-PE (P44-8, 352107, 1:40), CXCR6/CD186-PE-Cy7 (K041E5, 356012, 1:20), CD107a-BV421 (H4A3, 328626, 1:40)* von BioLegend. *CD103-PerCP-eFluor710 (Ber-ACT8, 46-1037-42, 1:40), CD7-APC-eFluor780 (eBio124-1D1, 47-0079-41,1:80)* von eBioscience. *CD94-FITC (REA113, 130-098-975, 1:40), NKG2A/CD159a-APC (REA110, 130-098-809, 1:40), NKp44/CD336-PE-Vio770 (2.29, 130-104-195, 1:40), KIR2D/CD158a-PE (NKVFS1, 130-092-688, 1:160), KIR3DL1/DL2/CD158e/k-PE (REA970, 130-095-205, 1:80), CD49a-APC-Vio770 (TS2/7,130-101-406, 1:40)* von Miltenyi Biotec. *hNKp80-APC (239127, FAB1900A, 1:40)* von R&D Systems. Für intrazelluläre Färbungen wurden oberflächengefärbte Zellen zunächst gewaschen und im Anschluss mit 1X *Cytofix-Reagenz* (eBioscience) inkubiert, erneut gewaschen und im Anschluss für 30 Minuten bei 4°C mit 1X *Cytoperm-Reagenz* (eBioscience) und den entsprechenden monoklonalen Antikörpern inkubiert. Die folgenden monoklonalen Antikörper (alle anti-human) wurden für die intrazellulären Färbungen verwendet: *T-bet-BV711 (4B10, 644819, 1:40), perforin-PerCP-Cy5.5 (d9G, 308114,1:40), IFN-γ-FITC (B27, 506504, 1:40), TNF-α-BV605 (MAb11, 502936, 1:40), granzyme B-FITC (GB11, 515403, 1:40)* von BioLegend. *Eomes-eFluor 660 (WD1928, 50-4877-42, 1:40)* von eBioscience. Das *Zombie Aqua™ Fixable Viability Kit* (BioLegend) wurde zur Bestimmung der Zellvitalität verwendet. Die gefärbten Zellen wurden innerhalb von 4 Stunden mittels des *BD LSRFortessa cell analyzer* (BD Biosciences) gemessen. Die erhobenen Daten

wurden mittels der *FlowJo-Software v10* (TreeStar, Ashland, Oregon, USA) ausgewertet.

Funktionelle Assays (NK-Zell-Degranulation/Zytokinproduktion)

Isolierte intestinale mononukleäre Zellen wurden in *IMDM*, versetzt mit 10% *FBS* resuspendiert und entweder unstimuliert belassen, mit *Phorbol-12-myristate 13-acetate* (*PMA*, Sigma-Aldrich) und *Ionomycin* (SantaCruz Biotechnology) stimuliert, oder mit *K562* oder *772.221* Zielzellen (Effektor/Zielzell-Quotient: 1:5) co-inkubiert.
Die Assays erfolgten unter Zugabe von *Brefeldin A* (Sigma Aldrich), *Monensin* (BD), sowie *anti-CD107a-BV421* (BioLegend) für jeweils 6 Stunden bei 37°C und 5% CO_2. Die *K562*-Zelllinie wurde von der Deutschen Sammlung von Mikroorganismen und Zellkulturen (DSMZ) bezogen. Die *772.221*-Zelllinie wurde von der America Type Culture Collection (ATCC) bezogen. Die Färbung intrazellulärer Zytokine erfolgte wie oben beschrieben. Die Werte der gemessenen Effektorparameter (CD107a, IFN-ɣ-, und TNF-α-positive Zellen) aus den stimulierten Kohorten wurden mit den korrespondierenden Werten der unstimulierten Kohorten wie folgt korrigiert:

$$relativer\ Wert = (\%positiv_{stimuliert} - \%positiv_{unstimliert}) * \frac{100\%}{(100\% - \%positiv_{unstimuliert})}$$

(Sagebiel et al., 2019)

Datenanalyse

GraphPad Prism 7 (GraphPad Software, San Diego, CA) wurde zur weiterführenden Datenauswertung und statistischen Analyse verwendet. Statistische Signifikanz der gemessenen Unterschiede wurde mittels non-parametrischen Mann-Whitney-U-Tests bzw. Wilcoxon-matched-pairs-signed-rank-Tests bei gepaarten Proben ermittelt. Wenn nicht anders angegeben, werden in Text und Abbildungen jeweils der Median der Prozentzahlen gemeinsam mit den jeweiligen Interquartilsabständen dargestellt. P-Werte < 0.05 wurden als signifikant erachtet. NK-Zellpopulationen wurden im Sinne einer Dimensionsreduktion mittels des Barnes–Hut-distributed stochastic neighbor embedding (bht-SNE oder viSNE) Algorithmus (Amir et al., 2013) ebenso wie SPADE-Clustering (Qiu et al., 2011) analysiert. Beide Algorithmen wurden von der Cytobank-Plattform (Cytobank Inc., Santa Clara, CA) zur Verfügung gestellt (Sagebiel et al., 2019).

Literaturverzeichnis

Alvarez, M., Bouchlaka, M. N., Sckisel, G. D., Sungur, C. M., Chen, M., & Murphy, W. J. (2014). Increased Antitumor Effects Using IL-2 with Anti–TGF-β Reveals Competition between Mouse NK and CD8 T Cells. *The Journal of Immunology*, *193*(4), 1709–1716. https://doi.org/10.4049/jimmunol.1400034

Amir, E. A. D., Davis, K. L., Tadmor, M. D., Simonds, E. F., Levine, J. H., Bendall, S. C., … Pe'Er, D. (2013). ViSNE enables visualization of high dimensional single-cell data and reveals phenotypic heterogeneity of leukemia. *Nature Biotechnology*, *31*(6), 545–552. https://doi.org/10.1038/nbt.2594

An, D., Oh, S. F., Olszak, T., Neves, J. F., Avci, F., Erturk-Hasdemir, D., … Kasper, D. L. (2014). Sphingolipids from a symbiotic microbe regulate homeostasis of host intestinal natural killer T cells. *Cell*, *156*(0), 123–133. https://doi.org/10.1016/j.cell.2013.11.042

Ardeshir, A., Narayan, N. R., Mendez-Lagares, G., Lu, D., Rauch, M., Huang, Y., … Hartigan-O'Connor, D. J. (2014). Breast-fed and bottle-fed infant rhesus macaques develop distinct gut microbiotas and immune systems. *Science Translational Medicine*, *6*(252), 252ra120. https://doi.org/10.1126/scitranslmed.3008791

Artis, D., & Spits, H. (2015). The biology of innate lymphoid cells. *Nature*, *517*(7534), 293–301. https://doi.org/10.1038/nature14189

Bernink, J. H., Krabbendam, L., Germar, K., de Jong, E., Gronke, K., Kofoed-Nielsen, M., … Spits, H. (2015). Interleukin-12 and -23 Control Plasticity of CD127^{+} Group 1 and Group 3 Innate Lymphoid Cells in the Intestinal Lamina Propria. *Immunity*, *43*(1), 146–160. https://doi.org/10.1016/j.immuni.2015.06.019

Bernink, J. H., Mjösberg, J., & Spits, H. (2017). Human ILC1: To Be or Not to Be. *Immunity*, *46*(5), 756–757. https://doi.org/10.1016/j.immuni.2017.05.001

Bernink, J. H., Peters, C. P., Munneke, M., te Velde, A. A., Meijer, S. L., Weijer, K., … Spits, H. (2013). Human type 1 innate lymphoid cells accumulate in inflamed mucosal tissues. *Nature Immunology*, *14*(3), 221–229. https://doi.org/10.1038/ni.2534

Björkström, N. K., Ljunggren, H.-G., & Michaëlsson, J. (2016). Emerging insights into natural killer cells in human peripheral tissues. *Nature Reviews Immunology*, *16*(5), 310–320. https://doi.org/10.1038/nri.2016.34

Caligiuri, M. A. (2008). Human natural killer cells. *Blood*, *112*(3), 461–469. https://doi.org/10.1182/blood-2007-09-077438

Calleja, S., Vivas, S., Santiuste, M., Arias, L., Hernando, M., Nistal, E., … Ruiz de Morales, J. G. (2011). Dynamics of non-conventional intraepithelial lymphocytes-NK, NKT, and gammadelta T-in celiac disease: relationship with age, diet, and histopathology. *Digestive Diseases and Sciences*, *56*(7), 2042–2049. https://doi.org/10.1007/s10620-010-1534-5

Cella, M., Gamini, R., Sécca, C., Collins, P. L., Zhao, S., Peng, V., … Colonna, M. (2019). Subsets of ILC3−ILC1-like cells generate a diversity spectrum of innate lymphoid cells in human mucosal tissues. *Nature Immunology*, *20*(8), 980–991. https://doi.org/10.1038/s41590-019-0425-y

Cepek, K. L., Shaw, S. K., Parker, C. M., Russell, G. J., Morrow, J. S., Rimm, D. L., & Brenner, M. B. (1994). Adhesion between epithelial cells and T lymphocytes mediated by E-cadherin and the αEβ7 integrin. *Nature*, *372*, 190. Retrieved from http://dx.doi.org/10.1038/372190a0

Cheroutre, H., Lambolez, F., & Mucida, D. (2011). The light and dark sides of intestinal intraepithelial lymphocytes. *Nature Reviews Immunology*, *11*(7), 445–456. https://doi.org/10.1038/nri3007

Coles, M. C., Veiga-Fernandes, H., Foster, K. E., Norton, T., Pagakis, S. N., Seddon, B., & Kioussis, D. (2006). Role of T and NK cells and IL7/IL7r interactions during neonatal maturation of lymph nodes. *Proceedings of the National Academy of Sciences*, *103*(36), 13457 LP – 13462. Retrieved from http://www.pnas.org/content/103/36/13457.abstract

Collins, A., Rothman, N., Liu, K., & Reiner, S. L. (2017). Eomesodermin and T-bet mark developmentally distinct human natural killer cells. *JCI Insight*, *2*(5), e90063. https://doi.org/10.1172/jci.insight.90063

Dalle, J. H., Menezes, J., Wagner, É., Blagdon, M., Champagne, J., Champagne, M. A., & Duval, M. (2005). Characterization of cord blood natural killer cells: Implications for transplantation and neonatal infections. *Pediatric Research*, *57*(5 I), 649–655. https://doi.org/10.1203/01.PDR.0000156501.55431.20

Diefenbach, A., Colonna, M., & Romagnani, C. (2017). The ILC World Revisited. *Immunity*, *46*(3), 327–332. https://doi.org/10.1016/j.immuni.2017.03.008

Dogra, P., Rancan, C., Ma, W., Fong, L., Lanier, L. L., & Farber, D. L. (2020). Tissue Determinants of Human NK Cell Development, Function, and Residence. *Cell*, *180*(4), 749-763.e13. https://doi.org/10.1016/j.cell.2020.01.022

Fan, H., Wang, A., Wang, Y., Sun, Y., Han, J., Chen, W., … Lu, Y. (2019). Innate Lymphoid Cells: Regulators of Gut Barrier Function and Immune Homeostasis. *Journal of Immunology Research*, *2019*, 2525984. https://doi.org/10.1155/2019/2525984

Fan, X., & Rudensky, A. Y. (2016). Hallmarks of Tissue-Resident Lymphocytes. *Cell*, *164*(6), 1198–1211. https://doi.org/10.1016/j.cell.2016.02.048

Fletcher, S., Van Hal, S., Andresen, D., McLaws, M.-L., Stark, D., Harkness, J., & Ellis, J. (2013). Gastrointestinal pathogen distribution in symptomatic children in Sydney, Australia. *Journal of Epidemiology and Global Health*, *3*(1), 11–21. https://doi.org/10.1016/j.jegh.2012.11.004

French, A. R., & Yokoyama, W. M. (2003). Natural killer cells and viral infections. *Current Opinion in Immunology 2003,* 45–51. https://doi.org/10.1016/S0952-7915(02)00002-X

Fuchs, A., Vermi, W., Lee, J. S., Lonardi, S., Gilfillan, S., Newberry, R. D., … Colonna, M. (2013). Intraepithelial type 1 innate lymphoid cells are a unique subset of IL-12- and IL-15-responsive IFN-γ-producing cells. *Immunity*, *38*(4), 769–781. https://doi.org/10.1016/j.immuni.2013.02.010

Gasteiger, G., Fan, X., Dikiy, S., Lee, S. Y., & Rudensky, A. Y. (2015). Tissue residency of innate lymphoid cells in lymphoid and nonlymphoid organs. *Science*, *350*(6263), 981–985. https://doi.org/10.1126/science.aac9593

Gasteiger, G., Hemmers, S., Firth, M. A., Le Floc'h, A., Huse, M., Sun, J. C., & Rudensky, A. Y. (2013). IL-2–dependent tuning of NK cell sensitivity for target cells is controlled by regulatory T cells. *The Journal of Experimental Medicine*, *210*(6), 1167 LP – 1178. Retrieved from http://jem.rupress.org/content/210/6/1167.abstract

Gebhardt, T., & Mackay, L. K. (2012). Local immunity by tissue-resident $CD8^+$ memory T cells. *Frontiers in Immunology*. https://doi.org/10.3389/fimmu.2012.00340

Hadley, G. A., & Higgins, J. M. G. (2014). Integrin alphaEbeta7: molecular features and functional significance in the immune system. *Advances in Experimental Medicine and Biology*, *819*, 97–110. https://doi.org/10.1007/978-94-017-9153-3_7

Hanna, J., Goldman-Wohl, D., Hamani, Y., Avraham, I., Greenfield, C., Natanson-Yaron, S., … Mandelboim, O. (2006). Decidual NK cells regulate key developmental processes at the human fetal-maternal interface. *Nature Medicine*, *12*, 1065. Retrieved from http://dx.doi.org/10.1038/nm1452

Hess, L. U., Martrus, G., Ziegler, A. E., Langeneckert, A. E., Salzberger, W., Goebels, H., Sagebiel, A. F., … Altfeld, M. (2020). The Transcription Factor Promyelocytic Leukemia Zinc Finger Protein Is Associated With Expression of Liver-Homing Receptors on Human Blood CD56^{bright} Natural Killer Cells. *Hepatology Communications*, *4*(3), 409—424. https://doi.org/10.1002/hep4.1463

Ivarsson, M. A., Loh, L., Marquardt, N., Kekäläinen, E., Berglin, L., Björkström, N. K., … Michaëlsson, J. (2013). Differentiation and functional regulation of human fetal NK cells. *The Journal of Clinical Investigation*, *123*(9), 3889–3901. https://doi.org/10.1172/JCI68989

Janssen, E. M., Lemmens, E. E., Wolfe, T., Christen, U., von Herrath, M. G., & Schoenberger, S. P. (2003). CD4^{+} T cells are required for secondary expansion and memory in CD8^{+} T lymphocytes. *Nature*, *421*(6925), 852–856. https://doi.org/10.1038/nature01441

Kim, K. S., Hong, S.-W., Han, D., Yi, J., Jung, J., Yang, B.-G., … Surh, C. D. (2016). Dietary antigens limit mucosal immunity by inducing regulatory T cells in the small intestine. *Science*, *351*(6275), 858–863. https://doi.org/10.1126/science.aac5560

Klose, C. S. N., & Artis, D. (2016). Innate lymphoid cells as regulators of immunity, inflammation and tissue homeostasis. *Nature Immunology*, *17*(7), 765–774. https://doi.org/10.1038/ni.3489

Koues, O. I., Collins, P. L., Cella, M., Robinette, M. L., Porter, S. I., Pyfrom, S. C., … Oltz, E. M. (2016). Distinct Gene Regulatory Pathways for Human Innate versus Adaptive Lymphoid Cells. *Cell*, *165*(5), 1134–1146. https://doi.org/10.1016/j.cell.2016.04.014

Krabbendam, L., Bernink, J. H., & Spits, H. (2021). Innate lymphoid cells: from helper to killer. *Current Opinion in Immunology*, *68*, 28–33. https://doi.org/https://doi.org/10.1016/j.coi.2020.08.007

Kramer, R. H., & Marks, N. (1989). Identification of integrin collagen receptors on human melanoma cells. *Journal of Biological Chemistry*, *264*(8), 4684–4688.

Lanier, L. L. (2005). NK cell recognition. *Annual Review of Immunology*, *23*(1), 225–274. https://doi.org/10.1146/annurev.immunol.23.021704.115526

Li, N., van Unen, V., Hollt, T., Thompson, A., van Bergen, J., Pezzotti, N., … Koning, F. (2018). Mass cytometry reveals innate lymphoid cell differentiation pathways in the human fetal intestine. *The Journal of Experimental Medicine*, *215*(5), 1383–1396. https://doi.org/10.1084/jem.20171934

Mackay, L. K., Braun, A., Macleod, B. L., Collins, N., Tebartz, C., Bedoui, S., … Gebhardt, T. (2015). Cutting Edge: CD69 Interference with Sphingosine-1-Phosphate Receptor Function Regulates Peripheral T Cell Retention. *The Journal of Immunology*, *194*(5), 2059–2063.

Mackay, L. K., Minnich, M., Kragten, N. A. M., Liao, Y., Nota, B., Seillet, C., … van Gisbergen, K. P. J. M. (2016). Hobit and Blimp1 instruct a universal transcriptional program of tissue residency in lymphocytes. *Science*, *352*(6284), 459–463. https://doi.org/10.1126/science.aad2035

Martrus, G., Goebels, H., Langeneckert, A. E., Kah, J., Flomm, F., Ziegler, A. E., … Altfeld, M. (2019). CD49a Expression Identifies a Subset of Intrahepatic Macrophages in Humans. *Frontiers in Immunology*, *10*, 1247. https://doi.org/10.3389/fimmu.2019.01247

Moretta, L., & Moretta, A. (2004). Unravelling natural killer cell function: Triggering and inhibitory human NK receptors. *EMBO Journal*. https://doi.org/10.1038/sj.emboj.7600019

Olszak, T., An, D., Zeissig, S., Vera, M. P., Richter, J., Franke, A., … Blumberg, R. S. (2012). Microbial Exposure During Early Life Has Persistent Effects on Natural Killer T Cell Function. *Science*, *336*(6080), 489–493. https://doi.org/10.1126/science.1219328

Panda, S. K., & Colonna, M. (2019). Innate Lymphoid Cells in Mucosal Immunity. *Frontiers in Immunology*, *10*, 861. https://doi.org/10.3389/fimmu.2019.00861

Phillips, J. H., Hori, T., Nagler, A., Bhat, N., Spits, H., & Lanier, L. L. (1992). Ontogeny of human natural killer (NK) cells: fetal NK cells mediate cytolytic function and express cytoplasmic CD3 epsilon,delta proteins. *The Journal of Experimental Medicine*, *175*(4), 1055–1066. Retrieved from http://jem.rupress.org/content/175/4/1055.abstract

Poggi, A., Benelli, R., Venè, R., Costa, D., Ferrari, N., Tosetti, F., & Zocchi, M. R. (2019). Human Gut-Associated Natural Killer Cells in Health and Disease. *Frontiers in Immunology*, *10*, 961. https://doi.org/10.3389/fimmu.2019.00961

Qiu, P., Simonds, E. F., Bendall, S. C., Gibbs, K. D., Bruggner, R. V, Linderman, M. D., … Plevritis, S. K. (2011). Extracting a cellular hierarchy from high-dimensional cytometry data with SPADE. *Nature Biotechnology*, *29*(10), 886–891. https://doi.org/10.1038/nbt.1991

Sagebiel, A. F., Steinert, F., Lunemann, S., Körner, C., Schreurs, R. R. C. E., Altfeld, M., … Bunders, M. J. (2019). Tissue-resident Eomes^{+} NK cells are the major innate lymphoid cell population in human infant intestine. *Nature Communications*, (2019), 1–13. https://doi.org/10.1038/s41467-018-08267-7

Salomé, B., Gomez-Cadena, A., Loyon, R., Suffiotti, M., Salvestrini, V., Wyss, T., … Jandus, C. (2019). CD56 as a marker of an ILC1-like population with NK cell properties that is functionally impaired in AML. *Blood Advances*, *3*(22), 3674–3687. https://doi.org/10.1182/bloodadvances.2018030478

Schreurs, R. R. C. E., Baumdick, M. E., Sagebiel, A. F., Kaufmann, M., Mokry, M., Klarenbeek, P. L., … Bunders, M. J. (2019). Human Fetal TNF-α-Cytokine-Producing CD4^{+} Effector Memory T Cells Promote Intestinal Development and Mediate Inflammation Early in Life. *Immunity*. https://doi.org/10.1016/j.immuni.2018.12.010

Schreurs, R. R. C. E., Drewniak, A., Bakx, R., Corpeleijn, W. E., Geijtenbeek, T. H. B., van Goudoever, J. B., & Bunders, M. J. (2017). Quantitative comparison of human intestinal mononuclear leukocyte isolation techniques for flow cytometric analyses. *Journal of Immunological Methods*, *445*, 45–52. https://doi.org/https://doi.org/10.1016/j.jim.2017.03.006

Schreurs, R. R. C. E., Sagebiel, A. F., Steinert, F. L., Highton, A. J., Klarenbeek, P. L., Drewniak, A., … Bunders, M. J. (2020). Intestinal CD8^{+} T cell responses are abundantly induced early in human development but show impaired cytotoxic effector capacities. *Manuskript akzeptiert in Mucosal Immunology 11/2020.*

Simoni, Y., Fehlings, M., Kløverpris, H. N., McGovern, N., Koo, S.-L., Loh, C. Y., … Newell, E. W. (2017). Human Innate Lymphoid Cell Subsets Possess Tissue-Type Based Heterogeneity in Phenotype and Frequency. *Immunity*, *46*(1), 148–161. https://doi.org/10.1016/j.immuni.2016.11.005

Sitrin, J., Ring, A., Garcia, K. C., Benoist, C., & Mathis, D. (2013). Regulatory T cells control NK cells in an insulitic lesion by depriving them of IL-2. *The Journal of Experimental Medicine*, *210*(6), 1153 LP – 1165. Retrieved from http://jem.rupress.org/content/210/6/1153.abstract

Spits, H., Artis, D., Colonna, M., Diefenbach, A., Di Santo, J. P., Eberl, G., … Vivier, E. (2013). Innate lymphoid cells — a proposal for uniform nomenclature. *Nature Reviews Immunology*, *13*(2), 145. https://doi.org/10.1038/nri3365

Spits, H., Bernink, J. H., & Lanier, L. (2016). NK cells and type 1 innate lymphoid cells: Partners in host defense. *Nature Immunology*. https://doi.org/10.1038/ni.3482

Stegmann, K. A., Robertson, F., Hansi, N., Gill, U., Pallant, C., Christophides, T., … Maini, M. K. (2016). CXCR6 marks a novel subset of T-bet^{lo} Eomes^{hi} natural killer cells residing in human liver. *Scientific Reports*, *6*(April), 1–10. https://doi.org/10.1038/srep26157

Sundström, Y., Nilsson, C., Lilja, G., Kärre, K., Troye-Blomberg, M., & Berg, L. (2007). The expression of human natural killer cell receptors in early life. *Scandinavian Journal of Immunology*, *66*(2–3), 335–344. https://doi.org/10.1111/j.1365-3083.2007.01980.x

Tang, L.-C., Xu, X.-H., & Jin, L.-P. (2020). Molecular characteristics and possible functions of innate lymphoid cells in the uterus and gut. *Cytokine & Growth Factor Reviews*, *52*, 15–24. https://doi.org/10.1016/j.cytogfr.2019.11.003

Thome, J. J. C., Bickham, K. L., Ohmura, Y., Kubota, M., Matsuoka, N., Gordon, C., … Farber, D. L. (2016). Early-life compartmentalization of human T cell differentiation and regulatory function in mucosal and lymphoid tissues. *Nature Medicine*, *22*(1), 1–7. https://doi.org/10.1038/nm.4008

Trowsdale, J., & Moffett, A. (2008). NK receptor interactions with MHC class I molecules in pregnancy. *Seminars in Immunology*. https://doi.org/10.1016/j.smim.2008.06.002

Vivier, E., Artis, D., Colonna, M., Diefenbach, A., Di Santo, J. P., Eberl, G., … Spits, H. (2018). Innate Lymphoid Cells: 10 Years On. *Cell*, *174*(5), 1054–1066. https://doi.org/10.1016/j.cell.2018.07.017

Vivier, E., Nunes, J. A., & Vely, F. (2004). Natural killer cell signaling pathways. *Science*, *306*(5701), 1517–1519. https://doi.org/10.1126/science.1103478

Weizman, O.-E., Adams, N. M., Schuster, I. S., Krishna, C., Pritykin, Y., Lau, C., … O'Sullivan, T. E. (2017). ILC1 Confer Early Host Protection at Initial Sites of Viral Infection. *Cell*, *171*(4), 795-808.e12. https://doi.org/10.1016/j.cell.2017.09.052

Yokoyama, W. M., & Plougastel, B. F. M. (2003). Immune functions encoded by the natural killer gene complex. *Nature Reviews Immunology*. https://doi.org/10.1038/nri1055

Abstract

Innate lymphoid cells (ILC), including natural killer (NK) cells, are implicated in host-defense and tissue-growth. However, the composition and kinetics of NK cells in the intestine during the first year of life, when infants are first broadly exposed to exogenous antigens, are still unclear. Here we show that $CD103^+$ NK cells are the major ILC population in the small intestines of infants. When compared to adult intestinal NK cells, infant intestinal NK cells exhibit a robust effector phenotype, characterized by Eomes, perforin and granzyme B expression, and superior degranulation capacity. Absolute intestinal NK cell numbers decrease gradually during the first year of life, coinciding with an influx of intestinal $Eomes^+$ T cells; by contrast, epithelial $NKp44^+CD69^+$ NK cells with less cytotoxic capacity persist in adults. In conclusion, NK cells are abundant in infant intestines, where they can provide effector functions while $Eomes^+$ T cell responses mature (Sagebiel et al., 2019).

Zusammenfassung

Natürliche Killerzellen (NK-Zellen) als Teil der Familie der Innate lymphoid cells (ILC) spielen eine entscheidende Rolle in der Verteidigung gegenüber viralen Infektionen aber auch bei der Entwicklung und Wachstum verschiedener Gewebe. Vor diesem Hintergrund waren die Zusammensetzung und Dynamiken intestinaler NK-Zellpopulationen bei Neugeborenen bislang unklar. Diese Periode der Entwicklung ist von besonderem Interesse, da in diesem Intervall ein rasches Wachstum, bakterielle Kolonisation, sowie die erstmalige Exposition gegenüber exogenen Antigenen erfolgt. In dieser Studie zeigen wir, dass $CD103^+$ NK-Zellen die größte ILC-Population im Dünndarm von Neugeborenen bilden. Insbesondere im Kontrast zu adulten Probanden zeigen intestinale NK-Zellen von Neugeborenen einen deutlichen Effektor-Phänotyp welcher sich durch eine hohe Eomes-, Perforin und Granzyme B-Expression auszeichnet und eine stärkere Degranulationskapazität als bei Erwachsenen aufweist. Die absoluten Zahlen jener intestinalen NK-Zellen zeigen sich in den verschiedenen Altersgruppen im ersten Lebensjahr schrittweise rückläufig. Jener Rückgang an NK-Zellen wird begleitet von einem Zuwachs an intestinalen $Eomes^+$ T-Zellen. Im Rahmen dessen verbleibt eine umschriebene Population an epithelialen $NKp44^+CD69^+$ NK-Zellen mit geringerer zytotoxischer Potenz bis hin ins Erwachsenenalter. Zusammenfassend lässt sich festhalten, dass in der Dünndarmmukosa von

Neugeborenen reichlich NK-Zellen vorzufinden sind, welche dort bereits früh in der Entwicklung immunologische Effektorfunktionen ausüben können, während T-Zellantworten des adaptiven Immunsystems noch heranreifen (Sagebiel et al., 2019).

Erklärung des Eigenanteils an der Publikation

Die Studie „*Wie Lymphozyten lernen sich zu benehmen*“ hinter der Publikation ist im Rahmen einer dreijährigen Anstellung als studentischer Mitarbeiter am Heinrich-Pette-Institut für Experimentelle Virologie in der Abteilung für Virus Immunologie unter der Leitung von Professor Marcus Altfeld entstanden und setzt sich bis heute fort.
Die Erstellung des Ethikantrages und der Aufklärungsbögen erfolgte gemeinsam von Dr. Dr. Madeleine Altfeld-Bunders (Betreuerin) und Adrian Sagebiel. Zu Beginn des Projekts erfolgte eine einmonatige Einarbeitung am Amsterdam University Medical Center in die Protokolle der Lymphozytenisolation durch Renée R.C.E. Schreurs. Die Etablierung jener Protokolle, sowie der klinischen Infrastruktur zur Probenakquirierung in Hamburg erfolgte durch Adrian Sagebiel unter Aufsicht von Dr. Dr. Altfeld-Bunders sowie Professor Konrad Reinshagen und Professor Daniel Perez für den klinischen Bereich. Die Probenakquirierung erfolgte nach Aufklärung durch die behandelnden Ärzte durch Adrian Sagebiel. Die Verarbeitung der Gewebeproben, Durchführung der Experimente, sowie Erhebung der durchflusszytometrischen Daten erfolgte für diese Publikation zum größten Teil durch Adrian Sagebiel, mit vereinzelt wechselseitiger Unterstützung durch Fenja Steinert und Renée R.C.E. Schreurs. Die Analyse der Daten und Erstellung der wissenschaftlichen Abbildungen erfolgte durch Adrian Sagebiel. Die Planung des Studiendesigns und der Experimente, die Interpretation der Daten, sowie Revision des Manuskripts erfolgte durch Dr. Dr. Altfeld-Bunders, Professor Marcus Altfeld und Adrian Sagebiel mit Unterstützung von Dr. Sebastian Lunemann und Dr. Christian Körner. Das Manuskript wurde von Adrian Sagebiel und Dr. Dr. Altfeld-Bunders mit Beiträgen aller Co-Autoren verfasst.

Danksagung

Mein Dank gilt in erster Linie den Patientinnen und Patienten, die diese Studie und meine damit verbundene Promotion erst ermöglicht haben. Insbesondere Eltern die vor dem Hintergrund bevorstehender Operationen Ihrer Kinder bereit waren sich Zeit zu nehmen, um die Grundlagenforschung zu unterstützen, bin ich sehr dankbar.
Darüber hinaus danke ich Dr. Dr. Madeleine Altfeld-Bunders und Professor Marcus Altfeld für die intensive Betreuung über die drei Jahre der Labortätigkeit. Weiterhin bin ich Renée R.C.E. Schreurs, Dr. Sebastian Lunemann, Dr. Christian Körner, Arne Düsedau, sowie Jana Hennesen für die Einarbeitung dankbar und dass ich sie jederzeit mit fachlichen Problemen konsultieren konnte.

Weiterhin möchte ich Professor Reinshagen und Professor Perez sowie den beteiligten Ober- und Assistenzärzten des UKE und AKK für die unkomplizierte und flexible Organisation und Unterstützung bei der Probenakquirierung danken.
Ich danke zudem meiner inzwischen Ehefrau Lischa Ohlde sowie meinen Eltern, die mich für die gesamte Zeit meines Studiums und insbesondere im Rahmen der Labortätigkeit am Heinrich-Pette-Institut jederzeit unterstützt haben.

Lebenslauf aus datenschutzrechtlichen Gründen entfernt.

Eidesstattliche Versicherung

Ich versichere ausdrücklich, dass ich die Arbeit selbständig und ohne fremde Hilfe verfasst, andere als die von mir angegebenen Quellen und Hilfsmittel nicht benutzt und die aus den benutzten Werken wörtlich oder inhaltlich entnommenen Stellen einzeln nach Ausgabe (Auflage und Jahr des Erscheinens), Band und Seite des benutzten Werkes kenntlich gemacht habe.
Ferner versichere ich, dass ich die Dissertation bisher nicht einem Fachvertreter an einer anderen Hochschule zur Überprüfung vorgelegt oder mich anderweitig um Zulassung zur Promotion beworben habe.
Ich erkläre mich einverstanden, dass meine Dissertation vom Dekanat der Medizinischen Fakultät mit einer gängigen Software zur Erkennung von Plagiaten überprüft werden kann.

Unterschrift: .....